NATIONAL RADIO ASTRONOMY OBSERVATORY
Charlottesville, Virginia
VERY LARGE ARRAY PROJECT

VLA Electronics Division Memo #128

November 1974

CIRCULAR TO RECTANGULAR WAVEGUIDE COUPLERS

C. Read Predmore

1. Circular to Rectangular Couplers

A microwave device is required which couples directly from the TE_{01} mode to 60 mm circular waveguide to the TE_{10} mode in rectangular waveguide[1]. Specifically, couplers in the frequency range 26 to 52 GHz are needed. In the remainder of this section a variety of possible coupling configurations are discussed, the coupler performance requirements are given, then the experimental results to date are summarized. The development of these couplers is on going, so the theory may be refined somewhat as various problems are encountered and more experimental results will be available.

Some of the theory and design details are presented in the appendices. Included are the phase matching of dissimilar waveguides, the coupling strengths of various apertures, and the normalized modes in circular waveguide.

1.1 Possible Coupling Configurations

As detailed in Appendix A the coupling between two adjoining waveguides is between the electric fields in each waveguide which are normal to the coupling aperture and between the tangential magnetic fields. Figure 1.1 shows the normalized longitudinal magnetic field (H_z) and the transverse electric and magnetic fields for the TE_{01} mode in 60 mm circular waveguide and for the TE_{10} mode in WR-28 rectangular waveguide (0.14x0.28"). As can be seen from the fields, longitudinal coupling between Hz fields can be accomplished by joining the narrow wall of the rectangular waveguide to the outer wall of the circular waveguide or by coupling in the center of the circular waveguide. Transverse coupling will be maximized when the center of the rectangular waveguide broad wall is joined to the circular waveguide fields at a point 0.485 of the distance from the center of the cylinder wall.

Although the rectangular waveguide cannot be introduced directly into the circular waveguide without producing a serious reflection, the circular waveguide can be split into two semi-circular waveguides with only a minor disturbance of the TE_{01} mode. The two semi-circular waveguides are then separated by a wedge until a rectangular waveguide can be interposed between the semi-circular waveguides. Examples of some various configurations are given in Figure 1.2 for longitudinal coupling and in Figure 1.3 for transverse coupling.

1.2 Coupler Performance

The 60 mm coupler requirements and specifications are given in Table 1.4 along with some experimental results for various coupling configurations.

1.2.1 Specifications

The TE_{01} insertion loss is limited since there will be fifteen (15) 60 mm couplers in the 21 km waveguide run in addition to nine (9) smaller diameter couplers. The TE_{01}^{o} return loss and TE_{01}^{o}-TE_{on}^{o} mode generation for a signal passing through the couplers has to be constrained since the reflections and spurious TE_{on}^{o} modes can seriously distort the transmitted signal. The fourth requirement for good TE_{on}^{o}(n>1) discrimination when the signal in the rectangular waveguide is coupled to the TE_{01}^{o} mode is needed only if other parts of the circular waveguide system (waveguide and joint diameter variations or tapers) can reconvert the TE_{on}^{o}(n>1) to the TE_{ol}^{o} mode.

The mode discrimination is not known for the experimental couplers but will be measured in the future. The required coupling and variation in coupling come from the allowable transmission loss and the maximum slope in a 50 MHz signal band. The coupler directivity is included to minimize the possibility of cross-talk between the millimeter channels.

1.2.2 Helical Longitudinal Coupler

The present designs for the helical coupler have good overall characteristics. The maximum coupling strength is limited to -26 to -28 dB since the TE_{01}^{o} magnetic field is weak at the wall and the apertures couple most of the power into other modes which can propagate in the smooth metal interior of the coupler. These other modes are quickly absorbed by the helix circular waveguide on each end of the coupler and do not usually present a problem. However, just at the frequency where a mode is cutoff[2] (or cutting on) there are very strong (3-10 dB) variations in the coupling. These can be moderated by introducing mode suppressors (such as a septum) into the circular

waveguide. Mode suppression techniques are now being investigated to minimize the coupling variation. An alternative magnetic coupler in the outer wall can be made by milling a slot in the wall of a piece of helix waveguide and introducing a rectangular waveguide for periodic coupling. The use of the mode-suppressing helix waveguide was suggested by Alan Parrish and is currently being fabricated.

Some preliminary results for a periodic coupler are included in Table 1.4 for a 10 slot coupler at 35 GHz. The coupling magnitude is what is expected from theory, but the spurious mode ripple was not much better than the helical coupler. This may be due to the intense Hz fields at the wall for TE_{nm} modes near cutoff. These fields would generate circumferential currents which would flow along the helix winding and not be absorbed.

1.2.3 Semi-Circular Transverse Coupler

This coupler has been discussed by Alan Parrish[3]. It offers stronger coupling than the outer wall couplers and with use of helix waveguide walls in the coupler section the coupling can be made quite smooth. However, the experimental coupler has a large insertion loss and strong TE_{01}-TE_{02} mode generation. Future work on this type and the center-fed magnetic coupler will aim to minimize the TE_{on} ($n>1$) effects of the semi-circular tapers and waveguide, while retaining the strong, smooth coupling.

In addition, the center-fed semi-circular coupler (Figure 1.2b) which discriminates against TE_{nm} ($n>0$) modes and TM_{nm} ($n>1$) modes will be investigated even though the Hz field at the center has a strength comparable to that at the outer wall (Figure 1.1a).

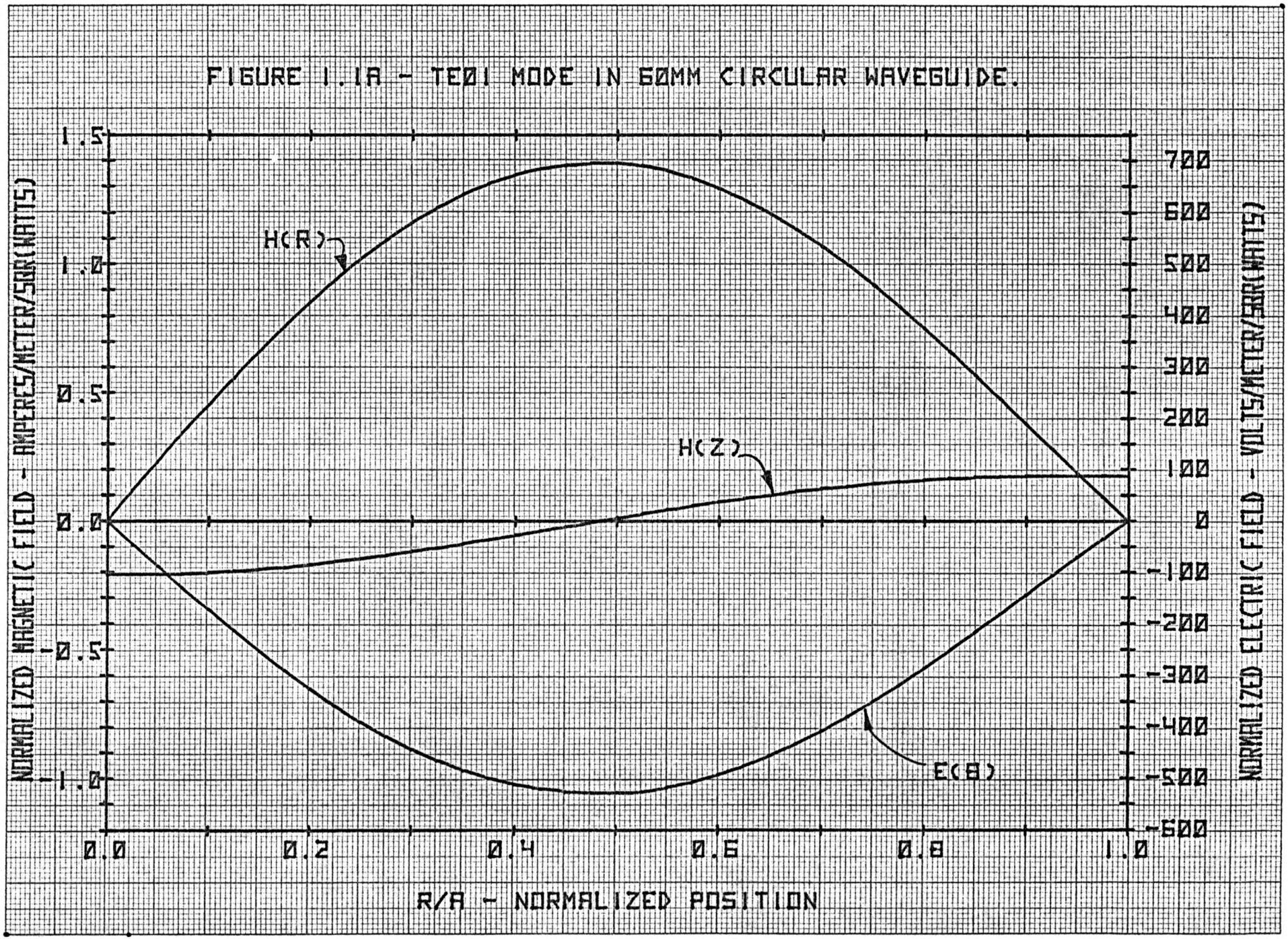
FIGURE 1.1A - TE01 MODE IN 60MM CIRCULAR WAVEGUIDE.
NORMALIZED MAGNETIC FIELD - AMPERES/METER/SQR(WATTS)
NORMALIZED ELECTRIC FIELD - VOLTS/METER/SQR(WATTS)
H(R)
H(Z)
E(θ)
1.5
1.0
0.5
0.0
-0.5
-1.0
700
600
500
400
300
200
100
0
-100
-200
-300
-400
-500
-600
0.0
0.2
0.4
0.6
0.8
1.0
R/A - NORMALIZED POSITION

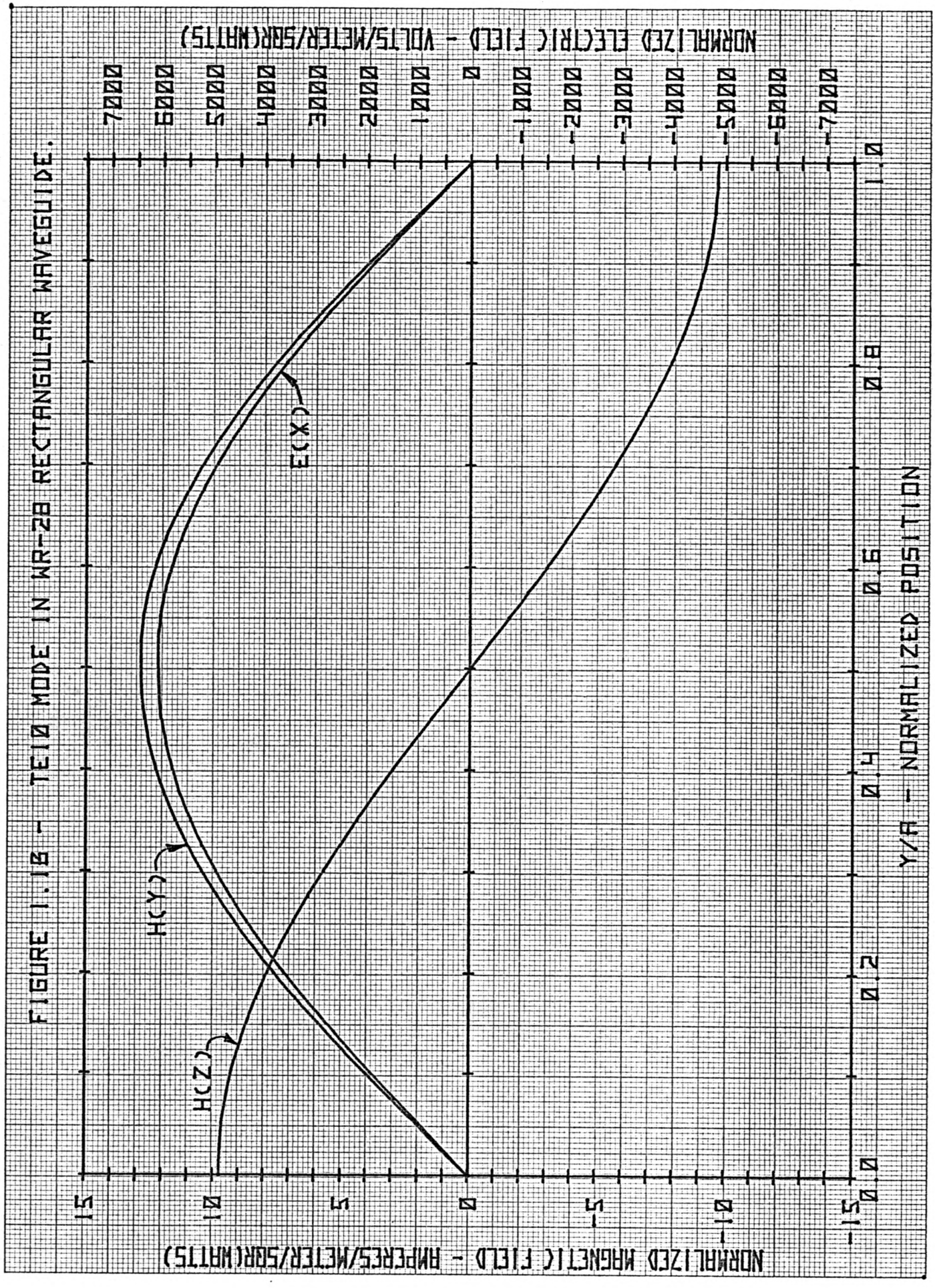

FIGURE 1.18 - TE10 MODE IN WR-28 RECTANGULAR WAVEGUIDE.

FIGURE 1.2 Longitudinal Magnetic Coupling

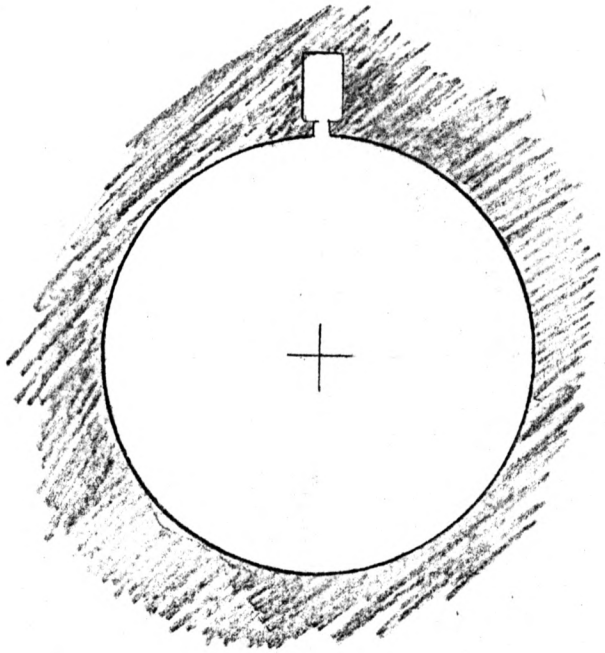

a) At outer wall of circular waveguide.

FIGURE 1.3 Transverse Magnetic and Electric Coupling

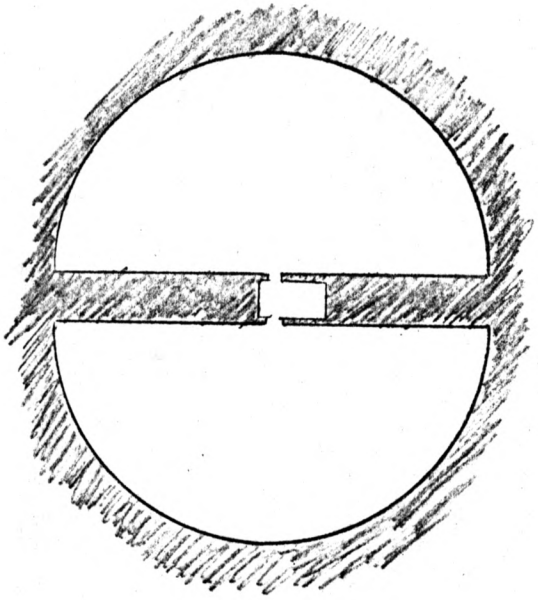

b) An axis of semi-circular waveguide.

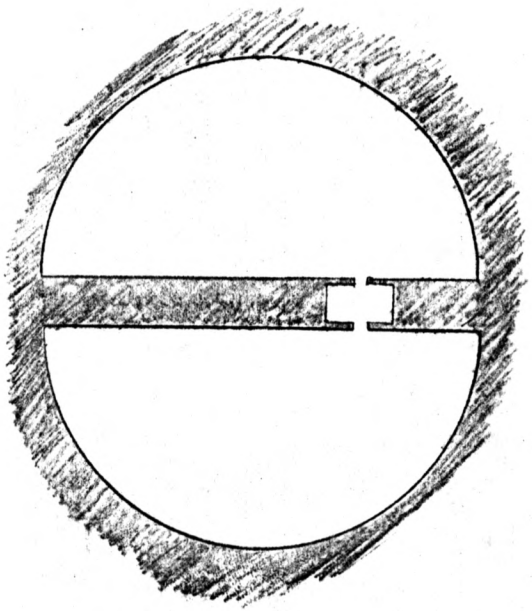

a) Off-axis in semi-circular waveguide.

TABLE 1.4

60 MM CIRCULAR WAVEGUIDE COUPLER

REQUIREMENT	SPECIFICATION	PRESENT RESULTS (October 1974)		
		Helix Coupler	Semi-Circular Transverse Coupler	Outer-Wall Periodic Coupler
1) TE°_{01} Insertion Loss	<0.10 dB	< 0.05 dB	1 dB*	Not known
2) TE°_{01} Return Loss	>50 dB	>40 dB	>40 dB	Not known
3) TE°_{on} Mode Generation in Circular Waveguide	<-40 dB	<-50 dB	<-12 dB*	Not known
4) TE°_{on} Mode Discrimination (n>1)	>20 dB	Not known	Not known	Not known
5) TE°_{01} - $TE^{\square}_{10}$ Coupling	-25 dB	-32 dB	-25.5 dB	-40 dB*
6) Coupling Variations				
a) Over 1 GHz	<1.0 dB	<3 dB*	1.5 dB	2-5 dB*
b) Over 50 MHz	<0.5 dB	<1 dB*	0.5 dB	0.5-5 dB*
7) $TE^{\square}_{10}$ Return Loss	>30 dB	>25 dB	15 dB*	5-20 dB*
8) Coupler Directivity	>20 dB	>20 dB	Not known	Not known

*These are preliminary values and will be improved.

APPENDIX A. Coupling Between Waveguides

The original theory for coupling between waveguides with a small hole ($d<<\lambda$) in a common wall was developed by Bethe[4] for circular and elliptical shapes. Cohn[5,6] made measurements for a variety of other shapes and extended[7] the theory to the case of large apertures ($d \approx \lambda$) and finite wall thickness. The best account of the theory which is readily available is by Collin[8]. There is also a good summary in the microwave design book by Matthaei, Young, and Jones[9] (Section 5.10). The coupling can be due to both the normal electric fields and the tangential magnetic fields which couple from one waveguide to the next and reflect a portion of the incident wave within the first waveguide. Figure A.1. shows the geometry of the fields on each side of the coupling hole. The net coupling for a single aperture is:

$$C = \frac{j\omega}{2} \left[\mu_o \left(H_{X1} M_X H_{X2} + H_{Y1} M_Y H_{Y2}\right) - \varepsilon_o E_{N1} P E_{N2}\right]$$

Figure A.2. is from reference 7 and shows the electric and magnetic dipoles induced in an aperture between two parallel-plane transmission lines.

The coupling is dependent on the normalized fields in the two waveguides and the magnetic (M) and electric (P) polarizabilities of the aperture. The normalized fields in circular waveguides are detailed in Appendix C while the normalized field for the $TE_{10}^{\square}$ is given below for the transverse fields in the xy plane and the z axis along the waveguide axis.

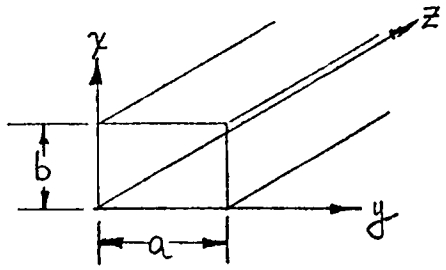

$$E_x = \left(\frac{2\omega\mu_o}{ab\ \beta_{10}}\right)^{1/2} \sin(\pi y/a),$$

$$Hy = \left(\frac{2\beta_{10}^{\square}}{ab\ \mu\omega_o}\right)^{1/2} \sin(\pi y/a),$$

$$Hz = \left(\frac{2}{ab\ \omega\mu_o\ \beta_{10}^{\square}}\right)^{1/2} \frac{\pi}{a} \cos(\pi x/a),$$

where a,b are the rectangular waveguide dimensions and $\beta_{10}^{\square} = 2\pi/\lambda g$ is the propagation constant.

The polarizabilities are proportional to the third power of the longest aperture dimension with values for a circle of

$$M = \ell^3/6$$

$$P = \ell^3/12$$

Figures A.3. and A.4. give the polarizabilities for other shapes and are from references 5, 6 and 9. For our design circles or slots are usually used. Once the polarizabilities are determined they are corrected for resonance and finite wall thickness.[7] When the parameters of an individual aperture are determined, then an array of slots are used to give broadband forward coupling, good coupling directivity and good match into all the coupling ports as discussed by Levy[12].

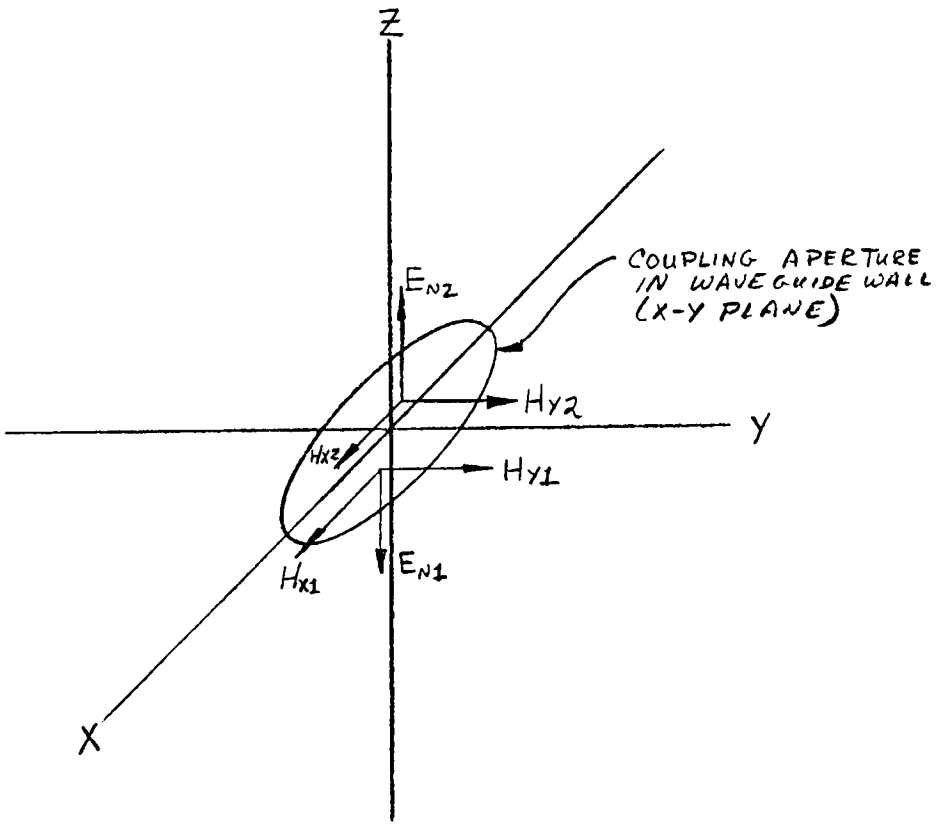

FIGURE A.1 - COUPLING BETWEEN WAVEGUIDES.

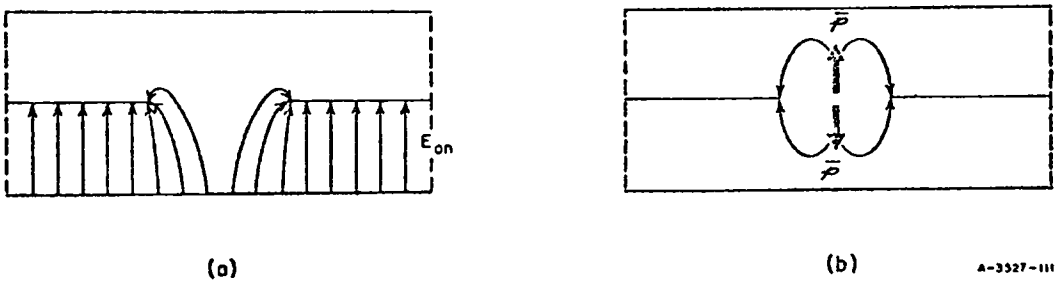

FIG. A.2 ELECTRIC DIPOLE MOMENTS INDUCED IN AN IRIS BY AN ELECTRIC FIELD NORMAL TO THE PLANE OF THE IRIS

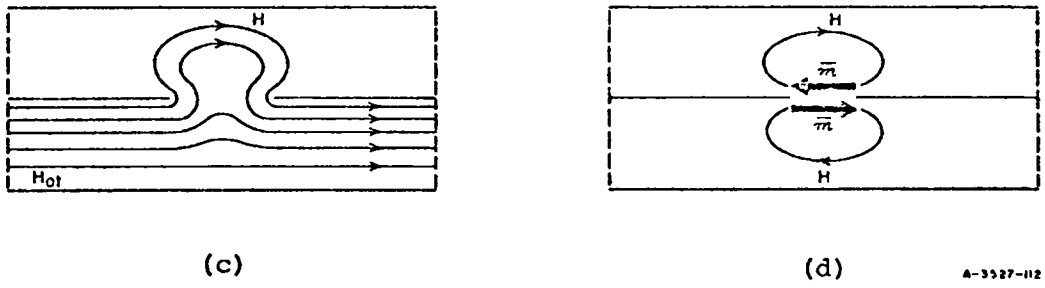

FIG. A.2 MAGNETIC DIPOLE MOMENTS INDUCED IN AN IRIS BY A MAGNETIC FIELD TANGENTIAL TO THE PLANE OF THE IRIS

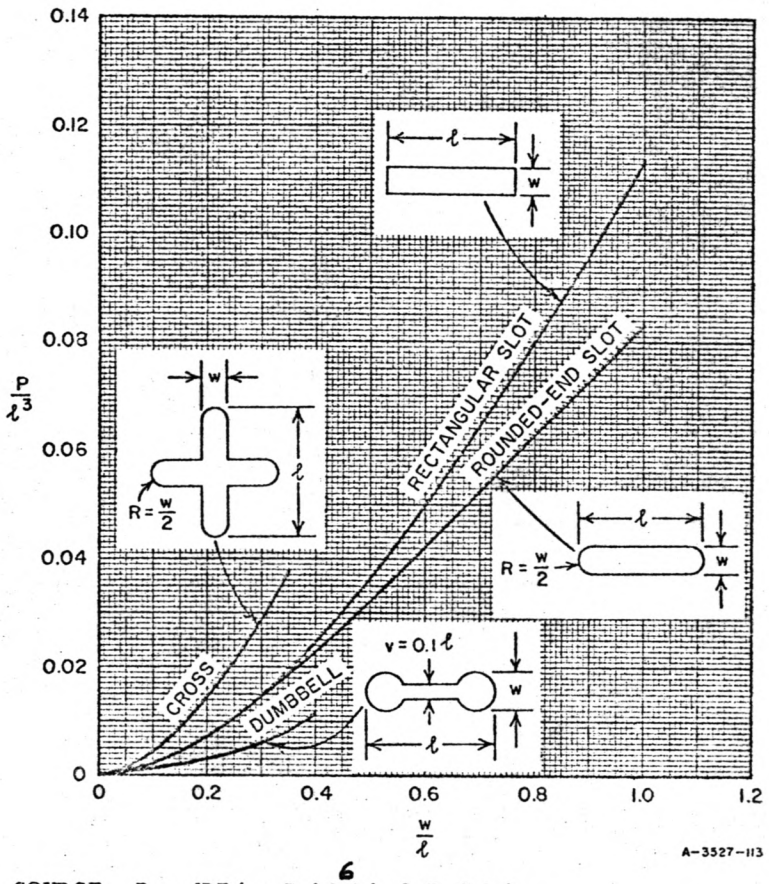

SOURCE: *Proc. IRE* (see Ref. 6, by S. B. Cohn).

FIG. A.3 MEASURED ELECTRIC POLARIZABILITIES OF RECTANGULAR, ROUNDED, CROSS- AND DUMBBELL-SHAPED SLOTS

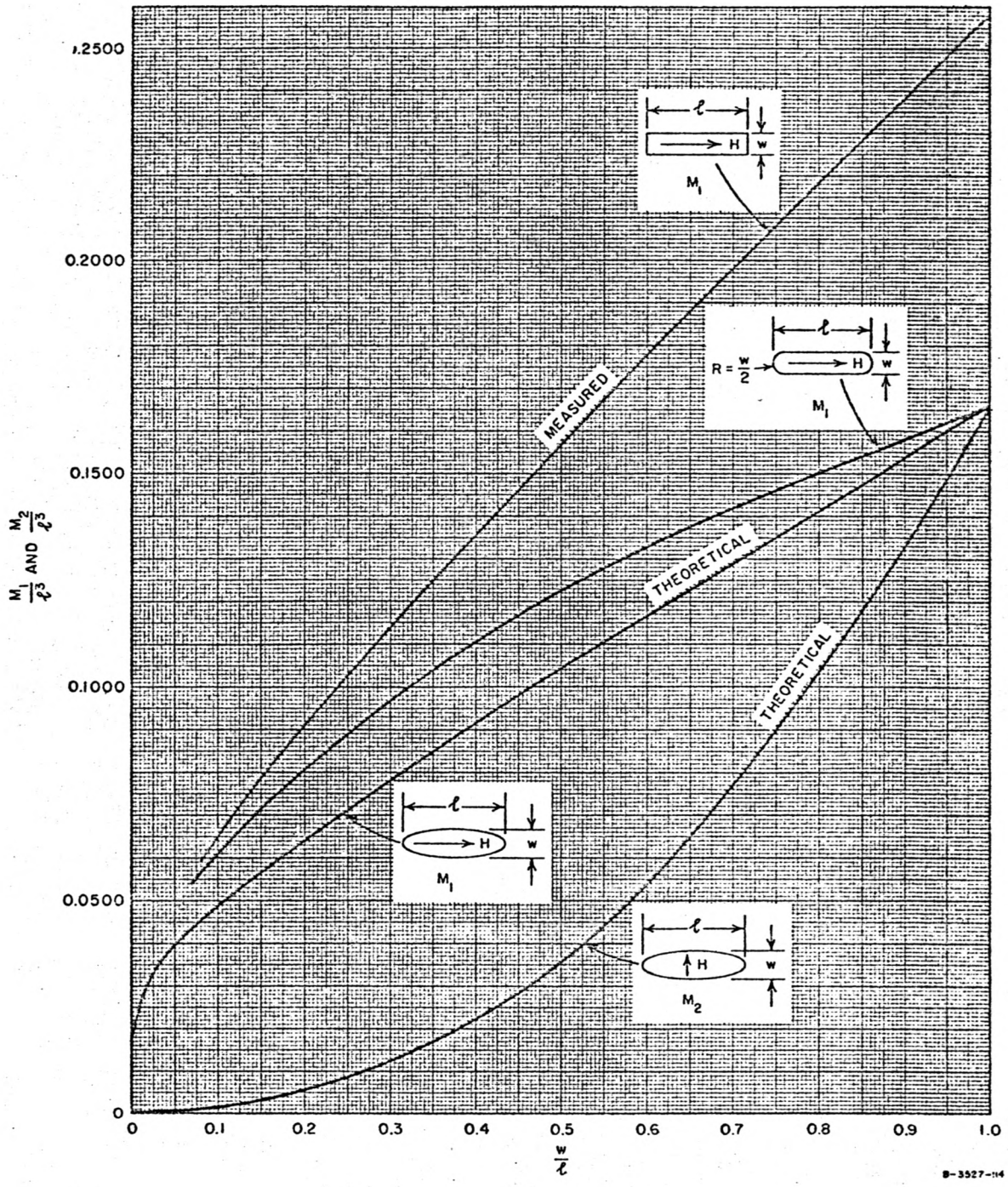

5

SOURCE: *Proc. IRE* (see Ref. ■, by S. B. Cohn).

FIG. A.4 MAGNETIC POLARIZABILITIES OF RECTANGULAR, ROUNDED-END, AND ELLIPTICAL SLOTS

APPENDIX B. Phase Matching

Since the TE_{01}^{o} mode in 60 mm waveguide has a cutoff frequency of 6.09 GHz and the two rectangular waveguide bands which cover 26-52 GHz have cutoff frequencies of 21.2 GHz (WR-28) and 31.4 (WR-19), the phase velocity in the circular waveguide will be lower than that in the rectangular waveguide. Figure B.1 shows the phase velocities for the TE_{10}^{o} and $TE_{10}^{\square}$ mode. The phase velocity can be lowered as shown by the dashed lines to bring the two phase velocities into step. If the phase velocities are used as they are coupling holes can be used a beat wavelength apart. These phase-matching techniques are examined below, then the bandwidths of the various methods are compared in the last section of this appendix.

B.1.1 Helical Coupler

If a rectangular waveguide is formed into a spiral about the cylindrical waveguide the phase-velocity of the rectangular waveguide is reduced by $\cos\theta = [1 + (\pi D_r/\ell)^2]^{-1/2}$, where D_r is the diameter on which the center of the rectangular waveguide lies, and ℓ is the pitch of the helix. Since the longitudinal magnetic fields in the two waveguides are now misaligned by the angle θ the voltage coupling coefficient is reduced by the factor $\cos\theta$. Figure B.2a and b show the spiral pitch for coupler in the range 26-40 GHz (WR-28 rectangular waveguide) and 40-60 GHz (WR-19). Figure B.2a shows the change of pitch for a $\pm$0.5 GHz change in f_{c2}, while Figure B.2b demonstrates the effect of the phase-shift ($\Delta\phi$) due to the coupling holes themselves. (In actual designs $\Delta\phi \approx 4°$.) The center signal frequencies of the VLA transmission system are marked on each graph. The remainder of this section discusses the tolerances required to fabricate the helical coupler.

For a given circular waveguide mode (f_{c1}) the center frequency of the helical coupler is determined by the cutoff frequency of the rectangular waveguide (f_{c2}), the lead of the spiral waveguide (ℓ) and the perturbation of the holes ($\Delta\phi$). They are related below:

First define:

$$\varepsilon_2 = \sqrt{1 + (\pi D_r/\ell)^2},$$

where D_r = diameter on which the center of the helix waveguide lies.

$$\varepsilon_2 \cdot \sqrt{f_o^2 - f_{c2}^2} = \sqrt{f_o^2 - f_{c1}^2} \cdot (1 - \Delta\phi/270°)$$

This gives a center frequency of

$$f_o = \frac{[((\varepsilon_2')^2 f_2^2 - f_1^2)]^{1/2}}{[((\varepsilon_2')^2 - 1)]^{1/2}}$$

where $\varepsilon_2' = \varepsilon_2/(1 - \Delta\phi/270°)$. By numerical differentiation at 35 GHz.

$$\frac{\partial f_o}{\partial(\Delta\phi)} = 0.23 \text{ GHz/degree}$$

$$\frac{\partial f_o}{\partial \ell_o} = 1.93 \text{ GHz/inch}$$

$$\frac{\partial f_o}{\partial f_2} = 1.81 \text{ GHz/GHz}$$

$$\frac{\partial f_o}{\partial f_1} = 0.18 \text{ GHz/GHz}$$

Since $\Delta f_1 < .02$ GHz from machining tolerances on the inside of the coupler, $\Delta f_o = \frac{\partial f_o}{\partial f_1} \cdot \Delta f_1 < 4$ MHz. This is negligible when compared to the other errors as shown below:

$$\Delta (\Delta\phi) = 1° \rightarrow \Delta f_o = 0.23 \text{ GHz}$$

$$\Delta \ell_o = .050" \rightarrow \Delta f_o = 0.096 \text{ GHz}$$

$$\Delta f_2 = 0.2 \text{ GHz} \rightarrow \Delta f_o = 0.36 \text{ GHz}$$

When combined in a root-mean-square fashion, the expected error is: $\Delta f_o = 0.39$ GHz, with the major contribution from the machining tolerances of the spiral groove which determine f_2.

B.1.2. Dielectric Loading

If the air of the second waveguide (f_{c2}) is replaced by a dielectric with relative permittivity $\varepsilon_r > 1$, then the cutoff frequency becomes $f_{c2}' = f_{c2}/\varepsilon_r$ and the phase velocity curve is lowered by a factor $(\varepsilon_r)^{-1/2}$. Phase matching is achieved at a frequency f_o where

$$f_o = \sqrt{(f_{c2}^2 - f_{c1}^2)/\sqrt{\varepsilon_r - 1}}$$

At 35 GHz when coupling from WR-28 rectangular waveguide ($f_{c2} = 21.2$ GHz) to the TE_{01} mode in 60 mm waveguide ($f_{c1} = 6.09$ GHz), the require permittivity is $\varepsilon_r = 1.337$. This is shown in Figure B.1. For a variation of 0.01 in ε_r the variation in f_o is

$$\Delta f = \frac{\partial f_o}{\partial E_r} \Delta E_r = 0.50 \text{ GHz}$$

In addition to the inaccuracy of the center frequency, the loss of the dielectric is quite a problem. At 35 GHz $\lambda_{g2} = \frac{299.7 \text{ (mm-GHz)}/\sqrt{\varepsilon_r}}{\sqrt{f_o^2 - (f_{c2}')^2}}$

$$= \frac{259.2}{29.81} = 8.67 \text{ mm}$$

$$\beta = \frac{2\pi}{\lambda_g} = 0.723 \text{ rad/mm}$$

$$\alpha = \beta \cdot \tan\delta = 2.2 \times 10^{-3} \text{ nepers/mm}$$

when $\tan \delta = 0.003$. For a coupler 12" (305 mm) long, $\alpha \ell = 0.671$ nepers → 5.9 dB. Measurements on Eccofoam S10, SH14, and S20 at 35 GHz gave losses of 6.4 dB, 7.5 dB and 9.0 dB in 12" This loss could be compensated for by enlarging the coupling apertures at the far end of the coupler but would still limit the coupling strength.

B.1.3 Periodic Loading in Waveguide

When the axes of the two waveguides are parallel, the waveguide with the lower cutoff frequency will have the most phase change between coupling holes. If the other waveguide is loaded (i.e. with a shunt susceptance) to produce additional phase shift, the two waveguides would then be phase matched.

$$\Delta\phi(\text{Loading}) = (\beta_1 - \beta_2) \cdot \ell - \Delta\phi(\text{holes})$$

At 35 GHz when coupling from WR-28 to 60 mm circular waveguide,

$$\Delta\beta = 7.92 \text{ degrees/mm},$$

$$\ell = 6.53 \text{ mm},$$

$$\Delta\phi(\text{holes}) = 4°,$$

then $\Delta\phi(\text{loading}) = 47.7°$.

However, the transmission phase shift of a single capacitve susceptance is limited to less than 19.5° (maximum at $jB = +1.4j$). This limitation and the required machining for a large number of capacitive posts has kept us from fabricating a periodic loaded coupler.

Possibly, some type of loading could be used with the periodic coupler discussed in Section B.2, to increase the number of coupling holes in a fixed coupler length.

B.2. Periodic Coupling

Periodic couplers have been extensively discussed by Miller[11] so only the necessary design equations are given here. Coupling arrays whose length is less than $\lambda_{Beat}/2$ are spaced a beat wavelength apart, where

$$\lambda_{Beat} = C/\left[\sqrt{f_o^2 - f_1^2} - \sqrt{f_o^2 - f_2^2}\right].$$

So once the individual arrays of holes are chosen (N=3-5) that array can be repeated indefinitely.

The periodic coupler is limited in the amount of coupling per unit length which can be achieved. However, in some cases it may be mechanically simpler to have a straight waveguide.

The bandwidth of a periodic coupler can be comparable to that of other phase-matched couplers as described in Section B.3.

B.3 Bandwidths of Phase-Matching Techniques

Since the coupling holes are usually the same size with a few smaller holes at each end of the array for matching purposes, the frequency response of an array of N holes is determined by

$$\frac{\text{Sin } (N\theta/2)}{N \text{ sin } (\theta/2)},$$

where $\theta = [(\beta_1 - \beta_2) \cdot S_1 - \Delta\phi]$

$\beta_{1,2}$ = propagation constants in the two waveguides

S_1 = hole spacing

$\Delta\phi$ = phase peturbation due to the coupling holes.

At the center frequency, $\theta = 0$ for a phase-matched coupler or $\theta_o = 360°$ for a periodic coupler. To find the 3 dB bandwidth of the coupler solve for θ such that

$$\frac{\text{Sin } (N\theta_3/2)}{N \text{ sin } (\theta_3/2)} = \frac{1}{\sqrt{2}}$$

For $N \geq 10$, $\theta_3 - \theta_o = \pm(160°/N)$

This can be used to find the $\Delta\beta = \beta_1 - \beta_2$ for a given hole spacing and number of holes, and then to solve for the corresponding bandwidth.

This is done in Table B.3 where helical, dielectric loaded and periodic couplers are compared. All of these have theoretical 3 dB bandwidths greater than 2 GHz so the other parameters for these couplers can be used to choose the best device for our application.

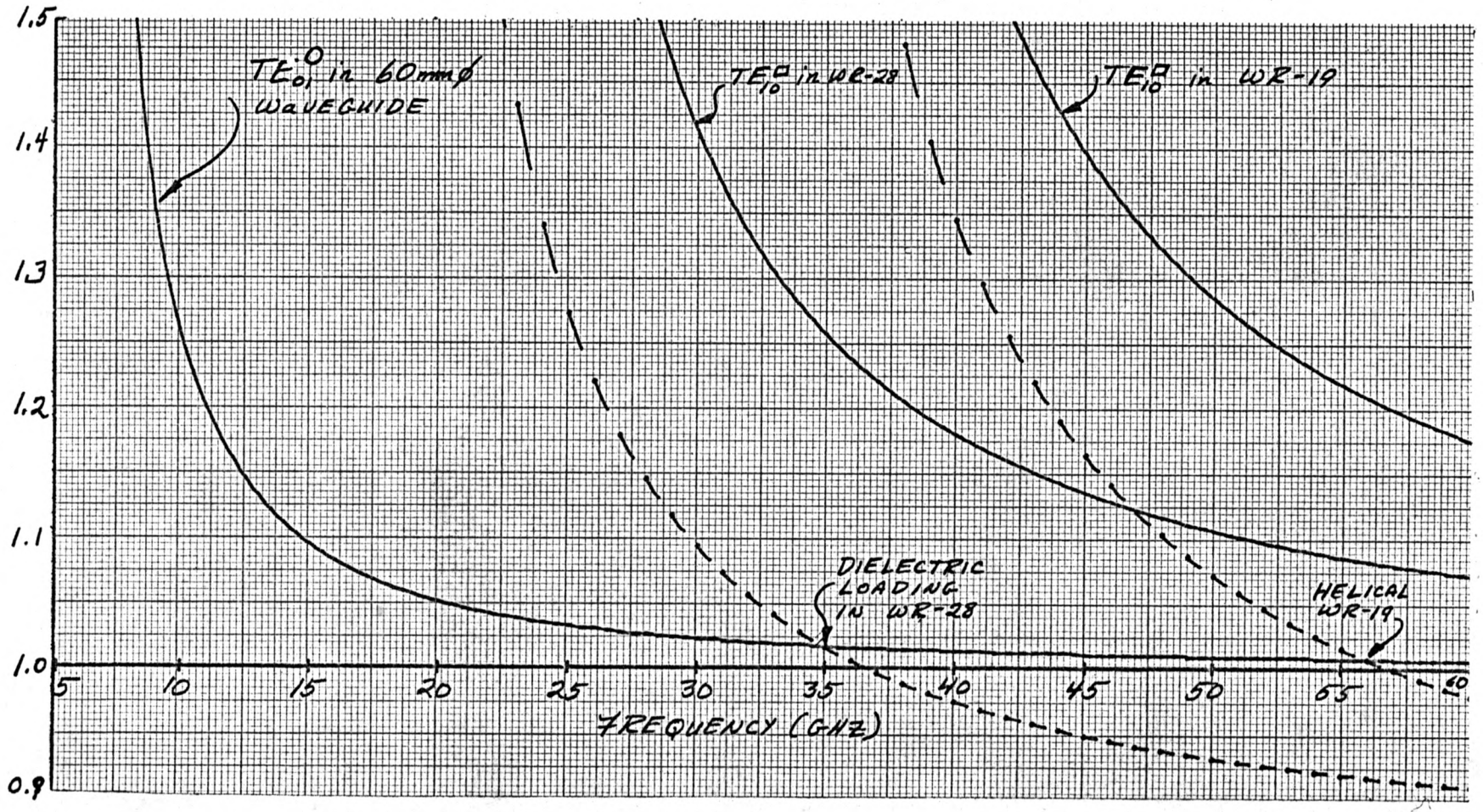
NORMALIZED PHASE VELOCITY (v_p/c)
1.5
1.4
1.3
1.2
1.1
1.0
0.9
5
10
15
20
25
30
35
40
45
50
55
60
FREQUENCY (GHZ)
TE_{01}^{o} in 60mm ϕ WAVEGUIDE
$TE_{10}^{\square}$ in WR-28
$TE_{10}^{\square}$ in WR-19
DIELECTRIC LOADING IN WR-28
HELICAL WR-19

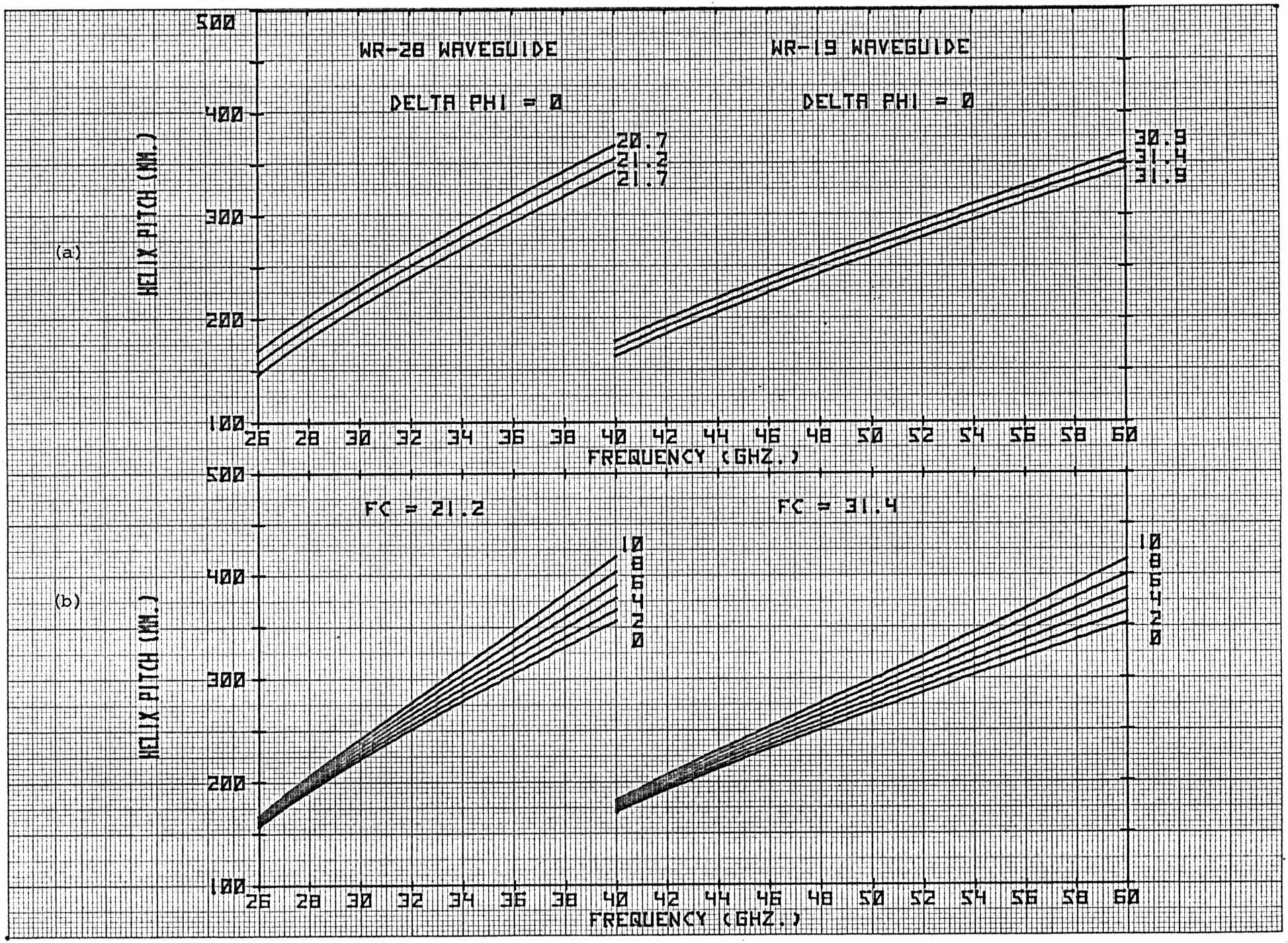
WR-28 WAVEGUIDE
DELTA PHI = 0
WR-19 WAVEGUIDE
DELTA PHI = 0
(a)
HELIX PITCH (MM.)
500
400
300
200
100
20.7
21.2
21.7
30.9
31.4
31.9
26 28 30 32 34 36 38 40 42 44 46 48 50 52 54 56 58 60
FREQUENCY (GHZ.)
FC = 21.2
FC = 31.4
(b)
HELIX PITCH (MM.)
10
8
6
4
2
0
FREQUENCY (GHZ.)

Figure B.2

TABLE B.3

COUPLER BANDWIDTHS

Phase-Matching Techniques	Typical Parameters at f_o=35 GHz Number of Holes	Total Length	Coupler 3 db Bandwidth (GHz)
I. Helix	40	260 mm	2.1 GHz
II. Dielectric Loading	40	260 mm	3.0 GHz
III. Periodic Coupling	12	550 mm	2.2 GHz

APPENDIX C. Normalized Modes in Circular Waveguide

Since the formulation of this problem follows that of Collin[8], his notation is used for the normalized modes. Collin has an excellent table (Table 5.5, p.197) which summarizes the mode properties in empty circular waveguide but does not give the explicit dependence of the electric and magnetic fields within the waveguide. The Waveguide Handbook by Marcavitz[10] does provide the field components for TE and TM modes in circular waveguide, but does not normalize the modes in the same manner as Collin.

Consequently the mode properties and normalized field components have been tabulated in Table C.2 for the TE modes and Table C.3 for the TM modes. The normalization used is that of Collin's equation 5.74a (p.201):

$$\iint_S \vec{e}_t \times \vec{h}_t \cdot a_z \, da = 1,$$

where $\vec{e}_t$ and $\vec{h}_t$ are the normalized electric and magnetic field vectors transverse to the waveguide axis and S is the waveguide cross sectional area.

Figure C.1 shows the r, θ, z, coordinate system and the waveguide cross section.

The fields given in Tables C.2 and C.3 are used to calculate the absolute coupling magnitude into any of the circular waveguide fields.

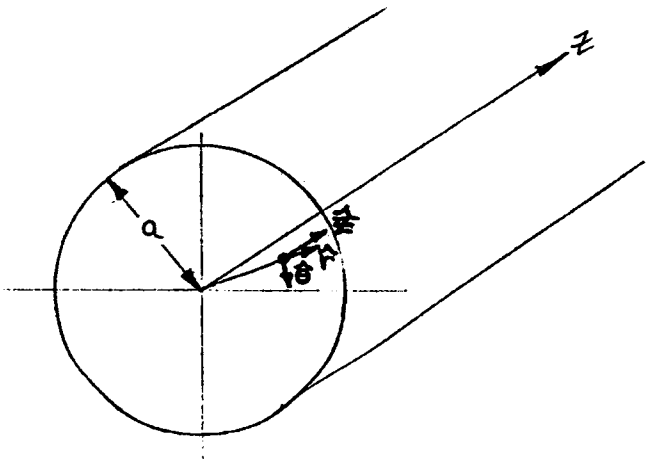

Figure C.1

TABLE C.2

NORMALIZED TE MODES IN CIRCULAR WAVEGUIDE

Cutoff wavelength $\lambda_c = 2\pi a/P_{nm}'$

where P_{nm}' = m^{th} root of $J_n'(x)$

Cutoff frequency $f_c = C\, P_{nm}'/(2\pi a)$

Free space wavelength $\lambda_o = c/f_o$

Guide wavelength $\lambda_g = (1/\lambda_o^2 - 1/\lambda_c^2)^{-1/2}$

Impedance of free space $Z_o = 377$ ohms/square

Define $R = \sqrt{(P_{nm}')^2 - n^2} \cdot J_n(P_{nm}')$

$\rho = P_{nm}' \cdot r/a,$

and $\varepsilon_n = \begin{cases} 1 \text{ if } n=0 \\ 2 \text{ if } n\neq 0 \end{cases}$

Normalized Fields

$$E_r = \pm\sqrt{\frac{\varepsilon_n \lambda_g Z_o}{\pi \lambda_o}} \frac{n \cdot J_n(\rho)}{r \cdot R} \begin{cases} \sin n\theta \\ \cos n\theta \end{cases}$$

$$E_\theta = \sqrt{\frac{\varepsilon_n \lambda_g Z_o}{\pi \lambda_o}} \frac{P_{nm}' \cdot J_n'(\rho)}{a \cdot R} \begin{cases} \cos n\theta \\ \sin n\theta \end{cases}$$

$$E_z = 0$$

$$H_r = -\sqrt{\frac{\varepsilon_n \lambda_o}{\pi \lambda_g Z_o}} \frac{P_{nm}' \cdot J_n'(\rho)}{a \cdot R} \begin{cases} \cos n\theta \\ \sin n\theta \end{cases}$$

$$H_\theta = \pm\sqrt{\frac{\varepsilon_n \lambda_o}{\pi \lambda_g Z_o}} \frac{n \cdot J_n(\rho)}{r \cdot R} \begin{cases} \sin n\theta \\ \cos n\theta \end{cases}$$

$$H_z = -j\sqrt{\frac{\varepsilon_n \lambda_o \lambda_g}{\pi \lambda_c^2 Z_o}} \frac{P_{nm}' \cdot J_n(\rho)}{a \cdot R} \begin{cases} \cos n\theta \\ \sin n\theta \end{cases}$$

TABLE C.3

NORMALIZED TM MODES IN CIRCULAR WAVEGUIDE

Cutoff wavelength $\lambda_c = 2\pi a/P_{nm}$

where $P_{nm} = m^{th}$ root of $J_n(x)$.

Cutoff frequency $f_c = c \cdot P_{nm}/(2\pi a)$

Guide wavelength $\lambda_g = (1/\lambda_o^2 - 1/\lambda_c^2)^{-1/2}$

Define $\rho = P_{nm} \cdot r/a$

Normalized Fields

$$E_r = -\sqrt{\frac{\varepsilon_n \lambda_o Z_o}{\pi \lambda_g}} \quad \frac{J_n'(\rho)}{a\, J_{n+1}(P_{nm})} \quad \begin{cases}\cos n\theta \\ \sin n\theta\end{cases}$$

$$E_\theta = \pm\sqrt{\frac{\varepsilon_n \lambda_o Z_o}{\pi \lambda_g}} \quad \frac{n\, J_n(\rho)}{P_{nm} \cdot r\, J_{n+1}(P_{nm})} \quad \begin{cases}\sin n\theta \\ \cos n\theta\end{cases}$$

$$E_z = -j\sqrt{\frac{\varepsilon_n \lambda_o \lambda_g}{\pi \lambda_c^2}} \quad \frac{J_n(\rho)}{a\, J_{n+1}(P_{nm})} \quad \begin{cases}\cos n\theta \\ \sin n\theta\end{cases}$$

$$H_r = \mp\sqrt{\frac{\varepsilon_n \lambda_g Z_o}{\pi \lambda_o Z_o}} \quad \frac{n\, J_n(\rho)}{P_{nm} \cdot r\, J_{n+1}(P_{nm})} \quad \begin{cases}\sin n\theta \\ \cos n\theta\end{cases}$$

$$H_\theta = -\sqrt{\frac{\varepsilon_n \lambda_g}{\pi \lambda_o Z_o}} \quad \frac{J_n'(\rho)}{a \cdot J_{n+1}(P_{nm})} \quad \begin{cases}\cos n\theta \\ \sin n\theta\end{cases}$$

$$H_z = 0$$

REFERENCES

[1] C. R. Predmore, VLA Electronics Memo #120 (Dec. 19, 1973) and addendum (August 8, 1974), "Loss and Coupling Values in the VLA Transmission System."

[2] R. W. Dawson, BSTJ, Vol. 36, 1957, p.391-408, "An Experimental Dual Polarization Antenna Feed for Three Radio Relay Bands."

[3] A. Parrish, VLA Electronics Memo #125, Oct. 1974, "Notes on Directional Couplers for 60 mm Circular Waveguide."

[4] H.A. Bethe, Physical Review, Vol. 66, p.163-182, "Theory of Diffraction by Small Holes", 1944.

[5] S. B. Cohn, Proc. I.R.E., Vol. 39, 1951, p.1416-21, "Determination of Aperture Parameters by Electrolytic Tank Measurements".

[6] S. B. Cohn, Proc. I.R.E., Vol. 40, 1952, p.1069-71, "The Electric Polarizability of Arbitrary Shape".

[7] S. B. Cohn, Proc. I.R.E., Vol. 40, 1952, p.696-699, "Microwave Coupling by Large Apertures".

[8] R. E. Collin, Field Theory of Guided Waves, 1960, McGraw-Hill, New York.

[9] G. L. Matthaei, L. Young and E. M. T. Jones, Design of Microwave Filters, Impedance-Matching Networks and Coupling Structures, Section 5.10, 1964, McGraw-Hill, New York, or National Technical Information Service, AD-402 852 (Vol. I) and AD-402 930 (Vol. II).

[10] N. Marcuvitz (ed.), Waveguide Handbook, 1951, p.66-72, McGraw-Hill, New York.

[11] S. E. Miller, BSTJ, Vol. 47, 1968, p.1801-1822, "On Solutions for Two Waves with Periodic Coupling."

[12] R. Levy, Advances in Microwaves (ed. by Leo Young), Vol. 1, 1966, p.115-211, "Direction Couplers", Academic Press, New York.

Helical Coupler from Rectangular-to-Circular Waveguide

C. READ PREDMORE, MEMBER, IEEE

Abstract—The very-large-array (VLA) radio telescope utilizes a low-loss TE_{01} circular waveguide transmission system. During the design of this system a coupler was developed which couples directly from a standard millimeter rectangular waveguide to the TE_{01}° mode in highly overmoded circular waveguide. In contrast to previous couplers which used periodically spaced groups of coupling holes, this design wraps the rectangular waveguide in a helix around the circular waveguide to give a continuous array of coupling apertures for maximum coupling and a compact mechanical configuration. The helix angle is chosen to match the phase velocities of the rectangular and circular waveguide modes at a given frequency. In particular, couplers have been designed and fabricated which couple from WR-28 (26.5–40-GHz) and WR-22 (33–50-GHz) rectangular waveguides to the TE_{01}^{c} mode in 20- and 60-mm-diam circular waveguide.

I. Introduction

THE very-large-array (VLA) radio telescope, presently being constructed near Socorro, NM, will combine the signals from 27 paraboloid antennas. The antennas are each 25 m in diameter and are arranged in a Y-shaped pattern to provide the optimum sky coverage [1]. Nine antennas will be placed on each arm of the Y at distances from 40 m to 21 km from the intersection of the three arms. There are 24 fixed locations on each arm for various observing configurations, with 14 of those stations being within 2 km of the center. All of the antennas on an arm are connected to the control building near the center of the array by a single TE_{01}° mode transmission system. This low-loss mode is achieved in a 60-mm-diam circular waveguide which has a helix lining of enameled copper wire for spurious mode suppression [2]–[4]. This waveguide mode has been studied for a number of decades [5] but has been brought to the production stage only recently in Japan and the United States [6].

Manuscript received February 4, 1976; revised May 14, 1976. This work was supported by Associated Universities, Inc., under contract with the National Science Foundation.

The author was with the National Radio Astronomy Observatory, Socorro, NM. He is now with the Department of Physics and Astronomy and the Department of Electrical and Computer Engineering, University of Massachusetts, Amherst, MA 01002.

Each antenna transmits local oscillator tones and a 200-MHz band received from astronomical sources to the control room in a 1-GHz band at a fixed frequency between 26 and 52 GHz. Weinreb *et al.* [7] describe the waveguide system in more detail. Since the losses in the circular waveguide are only 2.2–1.2 dB/km, between 26 and 52 GHz, the waveguide losses for the first 14 stations are less than 5 dB. Consequently, directional couplers with only loose coupling are required at those inner stations. It was desired to leave the couplers in place when the outer ten stations were being used. Since signals from those stations must propagate through the inner stations, the coupler insertion loss, return loss, and TE_{0n}° ($n > 1$) mode generation must be quite good. Section II discusses the desired characteristics for coupling into the 60-mm waveguide and matches the possible coupler types to the system requirements. In Section III the helical coupler design will be discussed. Then the experimental results for 20- and 60-mm helical couplers will be presented.

II. Design Criteria

The observing positions for the VLA antennas are clustered near the center of the Y with the first 14 stations within 2 km of the center. Beyond 2 km the spacing between stations increases from 400 m to 4 km. The waveguide loss is low so that no repeaters are required over the 21-km length. But, since the low loss does not dampen out interactions between system components such as couplers, which may be kilometers apart, the characteristics of the system components must be well chosen. Since the helix-lined waveguide will filter out TE_{mn}° ($m > 0$) and TM_{mn}° modes with a loss of >2000 dB/km, the prime considerations are the TE_{01}° return loss and the TE_{01}°–TE_{02}° mode generation for a wave going through a coupler.

A coupler with an inner diameter the same as the rest of the circular waveguide will minimize these quantities since reflections and TE_{0n}° ($n > 1$) mode generation are primarily caused by diameter changes [8]. Small-diameter couplers

Copyright © 1976 by The Institute of Electrical and Electronics Engineers, Inc.
Printed in U.S.A. Annals No. 611MT028

TABLE I
COUPLER COMPARISON

	Coupling Length (m)	Overall Length (m)	$TE_{10}^{\square}$-TE_{01}° Coupling (dB)	Coupling Variation in 1 GHz (dB)	TE_{01}° Insertion Loss* (dB)	TE_{01}° Return Loss (dB)	TE_{01}°-TE_{02}° Mode Generation (dB)	$TE_{01}^{\circ}/TE_{02}^{\circ}$ Mode Discrimination (dB)
Phase Matched Coupler	0.4	2.4	-3	1	0.5	25	-30	30
60 mm Diameter Periodic Coupler	1.2	1.8	-26to-34	3	0.05	50	-50	10
60 mm Diameter Beam Splitter Coupler	0.06	0.2	-3	1	0.2to0.6	35	-17to-27	17 to 27
20 mm Diameter Helical Coupler	0.4	2.5	-13to-24	2	0.5	30	-30	30
60 mm Diameter Helical Coupler	0.4	1.0	-24to-32	3	0.05	50	-50	10

*Not including coupled power loss.

require circular cross-sectional tapers from the small diameter to the 60-mm diameter of the waveguide system [9], [10]. These tapers generate TE_{02}° mode which can resonate between pairs of tapers in which the smaller diameter is cut off to the TE_{02}° mode [11].

In the past coupling from the $TE_{10}^{\square}$ to the TE_{01}° mode has been accomplished by making the waveguide dimensions such that the cutoff frequencies in the two waveguide modes are the same [12]. A circular waveguide diameter of 17.4 mm is required for phase matching to WR-28 (7.11 × 3.56 mm), and a 13.4-mm diameter is required for phase matching to WR-22 (5.59 × 2.79 mm) rectangular waveguide. If it was not possible to choose the waveguide dimensions to match the cutoff frequencies, it was still possible to use periodic coupling as described by Miller [13], [14]. However, for coupling between the axial magnetic fields, the number of coupling apertures in a given length is $1/\pi$ the number possible with a continuous coupling array. A third type of coupler is the quasi-optical beam splitter [15], [16] which consists of two 60-mm-diam waveguides which have a dielectric sheet at their intersection to couple out power by reflection. The helical coupler which wraps the rectangular waveguide around the circular waveguide in a spiral can be designed to phase match into any circular waveguide diameter which has a TE_{01}° cutoff frequency lower than the $TE_{10}^{\square}$ cutoff frequency.

These various couplers are compared in Table I which lists the actual coupling length and the overall length when the coupler is used in a 60-mm-diam system. Then the $TE_{10}^{\square}$-TE_{01}° coupling value and variation in coupling over the 1-GHz bandwidth required for the VLA are given. Next, the TE_{01}° insertion loss, the TE_{01}° return loss, and the TE_{10}°-TE_{02}° mode generation are listed. The final quantity in the table is the TE_{02}° mode discrimination, which is the ratio of the power coupled from the $TE_{10}^{\square}$ to TE_{01}° mode to the power coupled from the $TE_{10}^{\square}$ to TE_{02}° mode in the 1-GHz band centered on the coupler design frequency. For each of these couplers the $TE_{10}^{\square}$ return loss can be better than 23 dB and the coupler directivity better than 20 dB.

As can be seen from Table I, each type of coupler has different advantages which can be evaluated when selecting a coupler for a particular specification. While the phase-matched coupler which has a small diameter such as 13 mm and the beam-splitter coupler with a 60-mm diameter can couple as strong as −3 dB, they both have an unacceptable level of TE_{01}°–TE_{02}° mode generation for the inner couplers of the VLA system. This is caused by the tapers associated with the phase-matched coupler, which also add 2 m in length and additional cost to the coupler. The TE_{02}° mode generation is due to the intersecting 60-mm waveguide in the case of the beam splitter. This mode generation can be minimized at a particular frequency, but not over the octave band used in the VLA waveguide system [17]. A 60-mm-diam periodic coupler would have the required TE_{01}° return loss and TE_{01}°–TE_{02}° mode generation, but would have almost twice the overall length of the helical coupler and greater losses in the rectangular waveguide due to the longer length. The helical coupler offers the maximum coupling and most compact mechanical size in a 60-mm-diam coupler while achieving a high TE_{01}° return loss and a low TE_{01}°–TE_{02}° mode generation.

Beyond the inner 2 km of the VLA, stronger couplers are needed to compensate for the increasing waveguide loss. Phase-matched small-diameter couplers, 60-mm-diam beam-splitter couplers, and 20-mm-diam helical couplers are all being considered for the stronger coupling requirements.

III. Coupler Design

Once the circular waveguide diameter and channel frequencies are set by system requirements and the rectangular waveguide dimensions dictated by standard frequency bands, the number and size of the coupling apertures and the angle at which the rectangular waveguide is spiraled around the circular waveguide are determined. To optimize the VSWR and coupler directivity, the coupling slots are spaced an odd multiple of a quarter-wavelength apart along the axis of the circular waveguide. The arrangement of the coupling slots is shown in Fig. 1, which is a photograph of the helical coupler before the outer wall

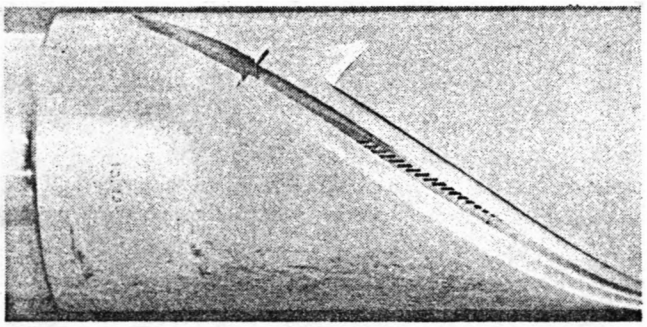

Fig. 1. Photograph of helical coupler from WR-28 to 60 mm. The outer cover of the rectangular waveguides has been left off to show the details of the coupling slots. At the end is a straight slot for adapting to standard WR-28 waveguide and a choke section for matching.

of the rectangular waveguide was fabricated. The helical coupler allows a continuous array of coupling apertures by machining a rectangular waveguide in a spiral around the circular waveguide. The narrow wall of the rectangular waveguide is common with the outer wall of the circular waveguide and the outer wall of the rectangular waveguide is fabricated in another step. The details of the design are discussed in the remainder of this section.

A. Multihole Coupling Arrays

The treatment of multihole coupling arrays given by Levy [18] for coupling between identical waveguides has been generalized to the case of coupling between dissimilar waveguides. The coupling arrays used in the helical coupler have a large number of identical apertures with three or four smaller slots at each end for matching purposes. Although these smaller slots are accounted for in the actual design, they are neglected in the following analysis. The total effect of the multihole coupling array is found for 1) the forward-coupled wave from the $TE_{10}^{\square}$ to the TE_{0n}° mode, 2) the reverse-coupled wave, and 3) for the reflected wave within the rectangular waveguide. The amplitudes for these three waves due to the coupling array are

$$A_1 = \sin [r \cdot (\phi_1 - \phi_2 - \varepsilon)/2]/\sin [(\phi_1 - \phi_2 - \varepsilon)/2] \tag{1}$$

$$A_2 = \sin [r \cdot (\phi_1 + \phi_2 + \varepsilon)/2]/\sin [(\phi_1 + \phi_2 + \varepsilon)/2] \tag{2}$$

and

$$A_3 = \sin [r \cdot (\phi_2 + \varepsilon)]/\sin (\phi_2 + \varepsilon) \tag{3}$$

where r is the number of coupling apertures, and ϕ_1,ϕ_2 are the electrical lengths along the circular waveguide axis between slots in the circular and rectangular waveguide, respectively. The phase shift in the rectangular waveguide due to the susceptance of the coupling aperture is typically 0.03 rad and is given by

$$\varepsilon = \tan^{-1} \rho \tag{4}$$

where ρ is the amplitude of the reflected wave in the rectangular waveguide as calculated in (9). The phase shift in the circular waveguide is negligible. The electrical lengths are given by

$$\phi_1 = 2\pi \cdot s/\lambda_g^{\circ} \tag{5a}$$

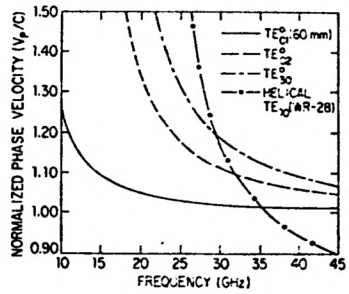

Fig. 2. Phase matching between the $TE_{10}^{\square}$ mode in helical WR-28 waveguide and the TE_{01}°, TE_{02}°, and TE_{03}° modes in 60-mm-diam circular waveguide. The cutoff frequencies for those modes are 21.2, 6.09, 11.2, and 16.2 GHz, respectively.

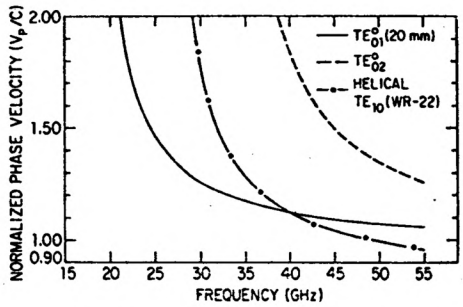

Fig. 3. Phase matching between the $TE_{10}^{\square}$ mode in helical WR-22 waveguide and the TE_{01}° and TE_{02}° modes in 20-mm-diam circular waveguide. The cutoff frequeocies for those modes are 26.7, 18.3, and 33.5 GHz, respectively.

and

$$\phi_2 = 2\pi \cdot s/(\lambda_g^{\square} \cdot \cos \theta). \tag{5b}$$

The guide wavelengths $\lambda_g^{\circ},\lambda_g^{\square}$ are for the TE_{0n}° and $TE_{10}^{\square}$ modes, the slot spacing is s, and the helix angle is θ. At the coupler center frequency f_0 the helix angle is chosen so that

$$\phi_1 = \phi_2 + \varepsilon \tag{6a}$$

or

$$\cos \theta = 1/\lambda_g^{\square} \cdot (1/\lambda_g^{\circ} - \varepsilon/2\pi s)^{-1} \tag{6b}$$

which reduces to

$$\cos \theta = \lambda_g^{\circ}/\lambda_g^{\square} \tag{6c}$$

when the phase shift ε is zero. This condition, which gives the maximum forward coupling, is illustrated in Fig. 2. This figure shows the phase matching of a WR-28 waveguide to a 60-mm-diam circular waveguide. The phase velocities versus frequency are plotted for the $TE_{10}^{\square}$, TE_{01}°, TE_{02}°, and TE_{03}° modes. The helix angle is chosen so that phase matching occurs at 35 GHz. Because of their higher cutoff frequencies, the rectangular waveguide is matched to the TE_{02}° and TE_{03}° modes at 32.5 and 27.8 GHz, respectively. The slot spacing along the circular waveguide axis is $\lambda_g^{\circ}/4$ at the center frequency. This makes

$$\phi_1 = \phi_2 + \varepsilon = \pi/2 \tag{7}$$

and minimizes the reverse-coupled wave (A_2) and the reflected wave (A_3) within the rectangular waveguide.

In Fig. 3 the phase matching of a WR-22 (5.6 × 2.8 mm) waveguide to 20-mm-diam circular waveguide is illustrated.

In this case the design frequency is 40 GHz. Also, for this design the $TE_{10}^{\square}$ cutoff frequency of 26.8 GHz is less than the TE_{02}° cutoff frequency of 33.5 GHz so that the rectangular waveguide is not phase matched to the TE_{02}° or higher TE_{0n}° modes at any frequency. This greatly decreases the coupling into the TE_{0n}° ($n > 1$) modes.

Since the coupling amplitude for a single slot does not vary rapidly with frequency, the bandwidth of the coupling is determined by the change in the electrical lengths ϕ_1, ϕ_2 as frequency varies and is expressed in (1). Even with the best calculations, a machined coupler may have errors of 1 percent in the peak coupling frequency f_0. At 35 GHz this shift is up to 20 percent of the 3-dB bandwidth. Fortunately, the coupler can be tuned to the correct frequency before the outer wall of the rectangular waveguide is fabricated. The tuning is accomplished by machining the outer wall of the cylinder in which the rectangular waveguide is milled. This decreases the rectangular waveguide width a and increases the cutoff frequency. As can be seen from Figs. 2 and 3, increasing the $TE_{10}^{\square}$ mode cutoff frequency increases the phase-matching frequency f_0. At 35 GHz, for the coupler described by Fig. 2, the tuning sensitivity is Δf_0 (GHz) = $9.4\Delta a$ (mm).

B. Calculation of Coupling Strength

The calculation of the coupling between two waveguides due to an aperture in a common wall follows that of Collin [19]. As shown in Fig. 1, the apertures are slots in the narrow wall of the rectangular waveguide with their longer dimension parallel to the axis of the circular waveguide. The magnetic polarizability for each slot, as well as the correction for the slot resonance frequency and finite wall thickness, are from the work of Cohn [20], [21]. The amplitude of the coupling between the $TE_{10}^{\square}$ and TE_{0n}° modes is given by

$$C = \frac{\omega\mu_0}{2} h_z^{\square}(M_l \cos\theta) h_z^{\circ}. \tag{8}$$

The amplitude of the reflection in the rectangular waveguide due to the coupling slot is given by

$$\rho = \frac{\omega\mu_0}{2} (h_z^{\square})^2 (M_l \cos^2\theta + M_W \sin^2\theta). \tag{9}$$

The longitudinal magnetic fields $h_z^{\square}$ and h_z° are the normalized fields at the coupling aperture for the modes being coupled and are given in the following equations:

$$h_z^{\square} = \left(\frac{2\lambda_0\lambda_g^{\square}}{abZ_0(\lambda_{10}^{\square})^2}\right)^{1/2} (\mathrm{Am^{-1}W^{-1/2}}) \tag{10}$$

$$h_z^{\circ} = \left(\frac{4\lambda_0\lambda_g^{\circ}}{\pi D^2 Z_0(\lambda_{0n}^{\circ})^2}\right)^{1/2} (\mathrm{Am^{-1}W^{-1/2}}). \tag{11}$$

The free-space wavelength is λ_0, the guide wavelengths for the rectangular and circular waveguide modes are $\lambda_g^{\square}$ and λ_g°, and the cutoff wavelengths are $\lambda_{10}^{\square}$ and λ_{0n}°, respectively. The rectangular waveguide width and height are a and b, respectively, and the circular waveguide diameter is D. The impedance of free space is $Z_0 = 377\ \Omega$.

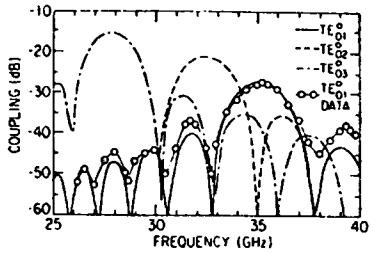

Fig. 4. Coupling between WR-28 and 60-mm-diam circular waveguide. The theoretical curves for the first three TE_{0n}° modes are shown.

The angular frequency is ω and μ_0 is the permeability of free space. The magnetic polarizabilities parallel and normal to the slot axis are M_l and M_w, respectively.

Once the reflection and coupling due to a single aperture are determined, the total effect of the 100 to 150 slots is found. The coupling C of (8) is multiplied by A_1, A_2 to determine the coupled amplitudes, while ρ of (9) is multiplied by A_3 for the reflected wave within the rectangular waveguide.

Coupling amplitudes for the three waves are calculated over the frequency range for the rectangular waveguide which is being used for the coupling. It is necessary to account for an additional factor in the design by including the loss of the coupling slots. Measurements on the actual loss due to coupling into the circular waveguide were made on the rectangular waveguide as a function of the slot resonance frequency, and an empirical formula was fitted to these data and applied to the calculation of the coupler response versus frequency.

C. Minimizing TE_{02} Coupling

All of the TE_{0n}° modes are circularly symmetric with only transverse currents on the wall, and consequently all of these modes have a low loss in the helix waveguide. Generation of both TE_{01}° and TE_{0n}° ($n > 1$) does not cause a problem until the TE_{0n}° ($n > 1$) modes are reconverted to the TE_{01}° mode by waveguide and joint diameter changes, or in other system components such as tapers between circular waveguides with different diameter (i.e., a 20–60-mm-diam taper).

Fig. 4 shows the theoretical coupling to the TE_{01}°, TE_{02}°, and TE_{03}° modes for WR-28 to 60-mm coupler. Also shown are the experimental results of a coupler fabricated from the design data. The theory gives a good fit to the main coupling peak and the frequencies of the coupling nulls but does not exactly predict the height of the sidelobes. By using pairs of couplers, the coupling peaks of the TE_{02}° and TE_{03}° modes have been measured and are within 3 dB of the theory.

As was indicated in Fig. 2, the peak of the TE_{02}° coupling occurs below the peak of the TE_{01} coupling, so the first null of the TE_{02}° coupling is positioned at the center frequency of the coupler to minimize the mode coupling.

If the electrical lengths between slots are calculated for the $TE_{10}^{\square}$ and TE_{02}° modes at the design frequency f_0, then the number of coupling slots r is chosen so that

$$r(\phi_1 - \phi_2 - \varepsilon) = \pm\pi. \tag{12}$$

Measurements of the beat between the TE_{01}° and TE_{02}° modes near f_0 indicate that the TE_{02}° mode discrimination is about 10 dB as expected although TE_{02}° generation in the tapers used is not known exactly. The TE_{03}° and higher TE_{0n}° modes are less of a problem since their reconversion to the TE_{01}° mode in tapers is at least 10 dB weaker than that due to the TE_{02}° mode and their losses in the circular waveguide are greater than 5 dB/km.

IV. Experimental Results

The design techniques discussed in the previous section were developed over a period of two years, with several iterations of couplers needed before the final design was settled. The primary difficulty was the shape and size of the coupling apertures. Initially, circular holes were tried but they had very strong resonances due to the excitation of spurious modes within the circular waveguide. Finally, slots with about a 4:1 length-to-width ratio were used. Although the coupled power increases as the sixth power of the slot length, there is also an increasing loss from power coupled into other circular waveguide modes. For coupling from WR-28 waveguide into 60-mm-diam waveguide, the optimum slot length is almost $3\lambda_0/8$ at the design frequency.

Table II summarizes the mechanical parameters for three helical couplers. Listed are the dimensions for the rectangular waveguide, the cutoff frequencies for the $TE_{10}^{\square}$ and TE_{01}° modes, and the design frequency. Next the helix angle and slot parameters are given. The slot parameters are the slot spacing, the total number of slots, and the slot length and width. Their actual coupling from the $TE_{10}^{\square}$ to the TE_{01}° mode is shown in Figs. 4, 5, and 6. The coupling shown in these figures was measured by using a swept backward-wave oscillator whose output went through a precision attenuation and a broad-band isolator, before going into a rectangular-to-circular waveguide transition and then a taper to 20- or 60-mm diameter as required. A short section of helix-lined circular waveguide was used as a mode filter before the coupler. The coupler was followed by a circular waveguide termination. The coupling was measured with the substitution technique by recording comparison curves at various attenuator settings and then recording the coupling with no attenuation.

The TE_{01}° insertion and return loss and the TE_{01}° to TE_{02}° mode generation listed in Table I were measured in a 60-mm-diam test line using the automatic waveguide test set developed by Weinreb *et al.* [7] and Parrish [22].

Fig. 5 shows the coupling response for a higher frequency coupler fabricated in WR-22 rectangular waveguide. The data from a 20-mm helical coupler are shown in Fig. 6. This coupler has stronger coupling because of the stronger h_z° fields in the 20-mm-diam waveguide, and has a broader bandwidth due to the small number of holes (50) and the small change in the differential electrical length $(\phi_1 - \phi_2)$ with frequency.

V. Conclusion

Couplers have been designed and fabricated to couple from the $TE_{10}^{\square}$ mode to the TE_{01}° or other TE_{0n}° modes in

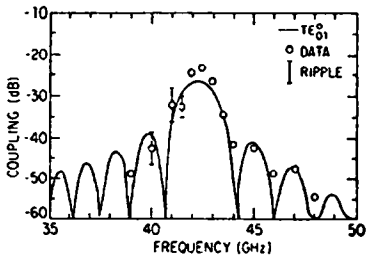

Fig. 5. Coupling between WR-22 and 60-mm-diam waveguide. The ripple below the peak coupling is due to a spurious mode.

TABLE II
Helical Coupler Parameters

	WR-28 to 60 mm Diameter	WR-22 to 60 mm Diameter	WR-28 to 20 mm Diameter
Rectangular Waveguide Dimensions a, b (mm)	7.11, 3.56	5.59, 2.79	7.11, 3.56
$TE_{10}^{\square}$ Cutoff Frequency (GHz)	21.2	26.8	21.2
TE_{01}° Cutoff Frequency (GHz)	6.09	6.09	18.3
Design Frequency (GHz)	35.1	42.3	40.0
Helix Angle θ	34.3°	36.6°	16.2°
Number of Slots	112	166	50
Slot Spacing (mm)	2.17	1.79	6.87
Slot Length (mm)	3.10	2.50	2.80
Slot Width (mm)	0.80	0.64	0.80

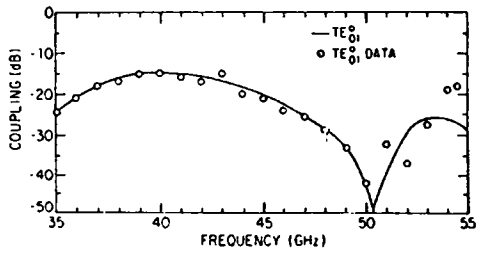

Fig. 6. Coupling between WR-28 and 20-mm-diam waveguide.

over-moded circular waveguide, over the octave band from 26 to 52 GHz. This design gives the maximum possible coupling, good directivity, excellent return loss, and a compact mechanical package. The theory can readily be extended to other frequencies and waveguide dimensions. Provision has been made to minimize the coupling to higher order TE_{0n}^{o} ($n > 1$) modes, or the coupler could be optimized as a TE_{0n}^{o} mode exciter for testing circular waveguide and circular waveguide components. With still smaller diameters, the helical couplers could be extended to stronger coupling and used as frequency-selective channel-dropping filters.

Acknowledgment

The author wishes to thank Dr. S. Weinreb of NRAO for his support of this work, and Dr. A. Parrish, J. E. Davis, and M. Ogai for valuable discussions and measurements. He also wishes to thank D. Dillon and W. Luckado for their help in fabrication of the prototype couplers.

References

[1] D. S. Heeschen, "The very large array," *Sky and Telescope*, vol. 49, pp. 344–351, June 1975.
[2] H. G. Unger, "Normal modes and mode conversion in helix waveguide," *Bell Sys. Tech. J.*, vol. 40, pp. 255–280, Jan. 1961.
[3] K. Noda, K. Yamaguchi, and N. Suzuki, "Circular electric wave transmission through helix waveguide," *Review of the Electrical Communication Laboratory*, vol. 10, pp. 49–70, Jan./Feb. 1962.
[4] D. T. Young and W. D. Warters, "Precise 50–60 GHz measurements on a two-mile loop of helix waveguide," *Bell Sys. Tech. J.*, vol. 48, p. 933, June 1968.
[5] S. E. Miller, "Waveguide as a communication medium," *Bell Sys. Tech. J.*, vol. 33, pp. 1209–1247, June 1954.
[6] T. A. Abele, D. A. Alsberg, and P. T. Hutchison, "A high-capacity digital communication system using TE_{01} transmission in circular waveguide," *IEEE Trans. Microwave Theory Tech.*, vol. MTT-23, pp. 326–333, April 1975.
[7] S. Weinreb, M. Ogai, A. Parrish, and R. Predmore, "Waveguide system for a very large antenna array," to be presented at the IEE International Conference on Millimetric Waveguide Systems, Nov. 9–12, 1976.
[8] H. E. Rowe and W. D. Warters, "Transmission in multimode waveguide with random imperfections," *Bell Sys. Tech. J.*, vol. 41, pp. 745–768, May 1962.
[9] C. C. H. Tang, "Optimization of waveguide tapers capable of multimode propagations," *IEEE Trans. Microwave Theory Tech.*, vol. MTT-9, pp. 442–452, Sept. 1961.
[10] H. G. Unger, "Circular waveguide taper of improved design," *Bell Sys. Tech. J.*, vol. 37, pp. 1599–1647, 1958.
[11] A. P. King and E. A. Marcatili, "Transmission loss due to resonance of loosely-coupled modes in a multi-mode system," *Bell Sys. Tech. J.*, vol. 35, pp. 899–906, 1956.
[12] A. P. King, "Status of low-loss waveguide and components at millimeter wavelengths," *Microwave J.*, vol. 7, pp. 102–106, March 1964.
[13] S. E. Miller, "Coupled wave theory and waveguide applications," *Bell Sys. Tech. J.*, vol. 33, pp. 661–719, May 1954.
[14] S. E. Miller, "On solutions for two waves with periodic coupling," *Bell Sys. Tech. J.*, vol. 47, pp. 1801–1822, Oct. 1968.
[15] E. A. Marcatili and D. L. Bisbee, "Band splitting filter," *Bell Sys. Tech. J.*, vol. 40, pp. 197–212, Jan. 1961.
[16] N. Suzuki, "A new band-splitting filter for guided-millimeter-wave transmission systems," *IEEE Trans. Microwave Theory Tech.*, vol. MTT-24, pp. 237–241, May 1976.
[17] M. Ogai, private communication.
[18] R. Levy, "Directional couplers," in *Advances in Microwaves*, vol. 1. New York: Academic Press, 1966, pp. 115–211.
[19] R. E. Collin, *Field Theory of Guided Waves*. New York: McGraw-Hill, 1960.
[20] S. B. Cohn, "Determination of aperture parameters by electrolytic tank measurements," *Proc. of the IRE*, vol. 39, pp. 1416–1421, Dec. 1951.
[21] S. B. Cohn, "Microwave coupling by large apertures," *Proc. of the IRE*, vol. 40, pp. 696–699, June 1952.
[22] A. Parrish, *Instruction Manual for VLA Circular Waveguide Test Set*, NRAO Report, Green Bank, WV, Sept. 1974.

REV.	DATE	DRAWN BY	APPRV'D BY	DESCRIPTION

PART NO.	CHANNEL	HELIX LEAD ±.020	CHOKE LENGTH A ±.005	COUPLER SLOT START "S" ±.020	SLOT RUNOUT (ANGLE) ∝ (±0°30')
D1331OM16-6	6	14.750	.200		29°30'
5	5				
4	4	12.340	.236		34°13'
3	3	11.280	.262		36°30'
2	2	10.860	.298		40°24'
D1331OM16-1	1				

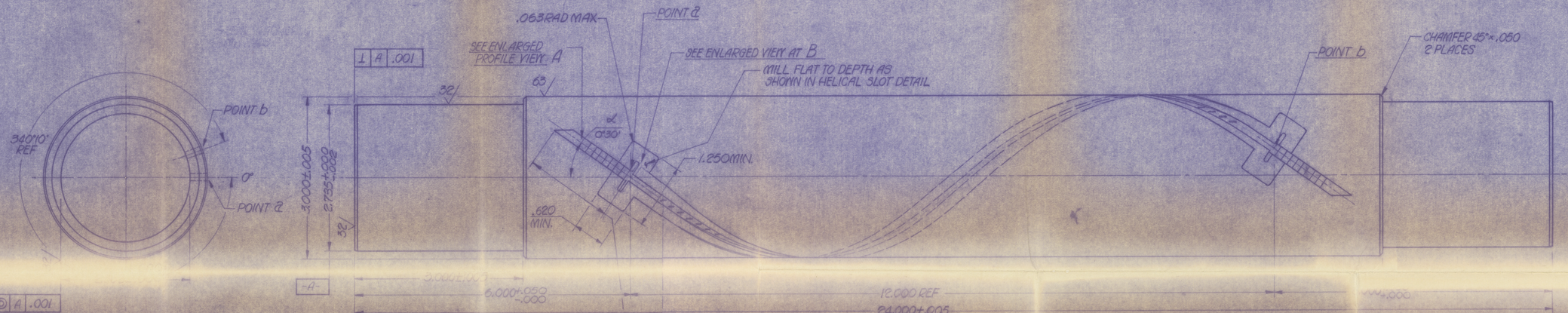

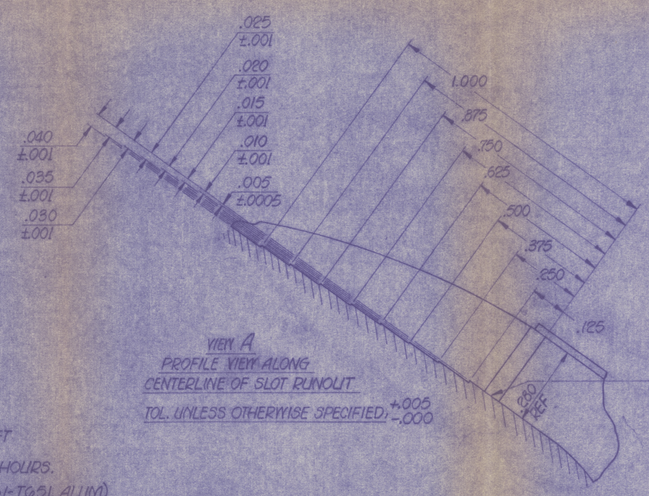

VIEW A
PROFILE VIEW ALONG CENTERLINE OF SLOT RUNOUT
TOL. UNLESS OTHERWISE SPECIFIED: +.005 -.000

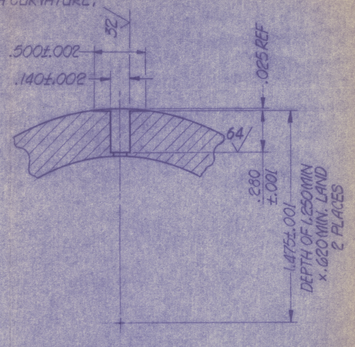

TYPICAL HELICAL SLOT DETAIL

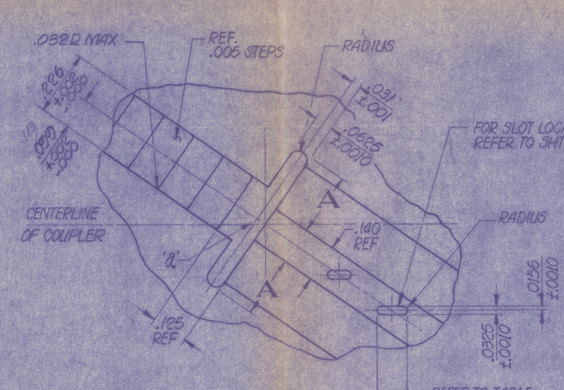

VIEW B
SCALE: 4/1

NOTES:
1. UNLESS OTHERWISE SPECIFIED, FILLET RADII TO BE .005 MAX.
2. STRESS RELIEVE AT 450°F FOR 8.0 HOURS.
3. MATERIAL TO BE CERTIFIED (6061-T651 ALUM)

NEXT ASSY	USED ON

UNLESS OTHERWISE SPECIFIED DIMENSIONS ARE IN INCHES
TOLERANCES: ANGLES ±
3 PLACE DECIMALS (.XXX): ±
2 PLACE DECIMALS (.XX): ±
1 PLACE DECIMALS (.X): ±

MATERIAL: MAKE FROM D1331OM11

FINISH:

REVISIONS

HELICAL COUPLER, ANTENNA STATION

NATIONAL RADIO ASTRONOMY OBSERVATORY
CHARLOTTESVILLE, VA. 22901

DRAWN BY	HARTLINE	DATE	6/75
DESIGNED BY		DATE	
APPROVED BY		DATE	

SHEET NUMBER | DRAWING NUMBER D1331OM16 | REV. | SCALE 1/1

BRUNING 40-22 24984

REV.	DATE	DRAWN BY	APPRV'D BY	DESCRIPTION

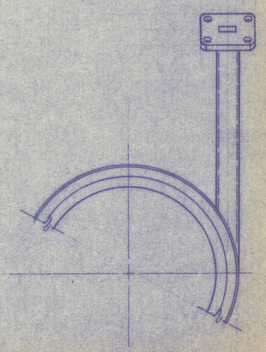

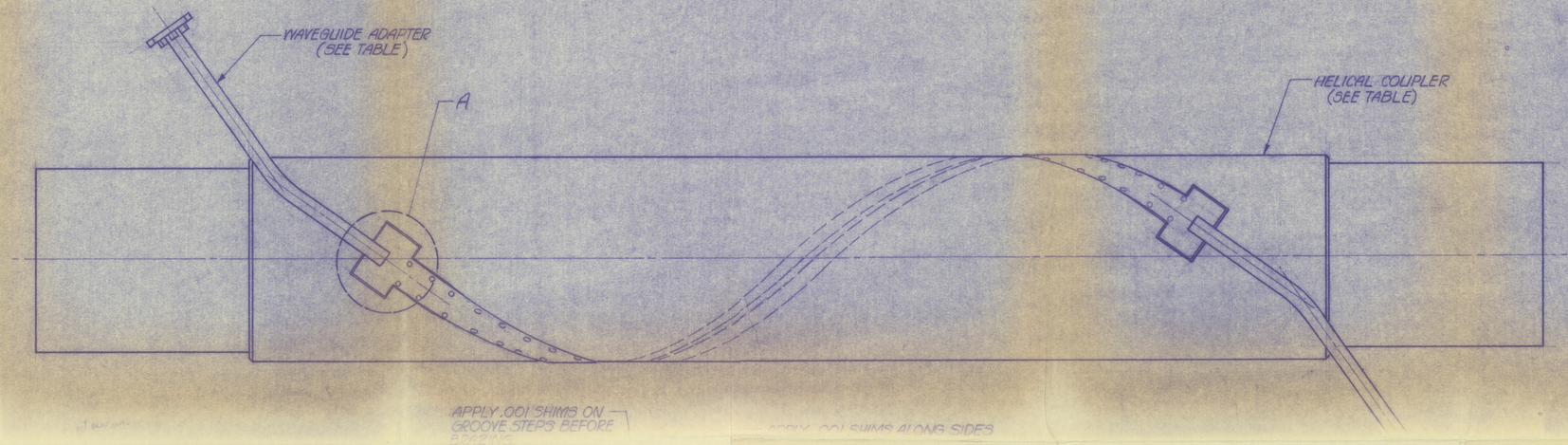

D1331OM25-11	D1331OM26-11	11	B1331OM20-5		UG-383/U
D1331OM25-10	-10	10	-4	13.88	
D1331OM25-9	-9	9	-3	14.14	
D1331OM25-8	-8	8	-2	14.51	
D1331OM25-7	D1331OM26-7	7	-1	15.00	UG-383/U
D1331OM25-6	D1331OM16-6	6	B1331OM20-6	13.77	UG-599/U
D1331OM25-5	-5	5	-5		
D1331OM25-4	-4	4	-4	14.61	
D1331OM25-3	-3	3	-3	15.13	
D1331OM25-2	-2	2	-2	16.07	
D1331OM25-1	D1331OM16-1	1	B1331OM20-1		UG-599/U
PART NO.	HELICAL COUPLER PART NO.	CHANNEL NO.	WAVEGUIDE (RECT.) ADAPTER PART NO.	COVER STRIP (LENGTH) *	WAVEGUIDE FLANGE PART NO.

* COVER STRIP, DWG. B1331OM17, ACTUAL LENGTH TO BE SIZED AT TIME OF COUPLER BRAZING. LENGTHS SHOWN ABOVE ARE APPROX.

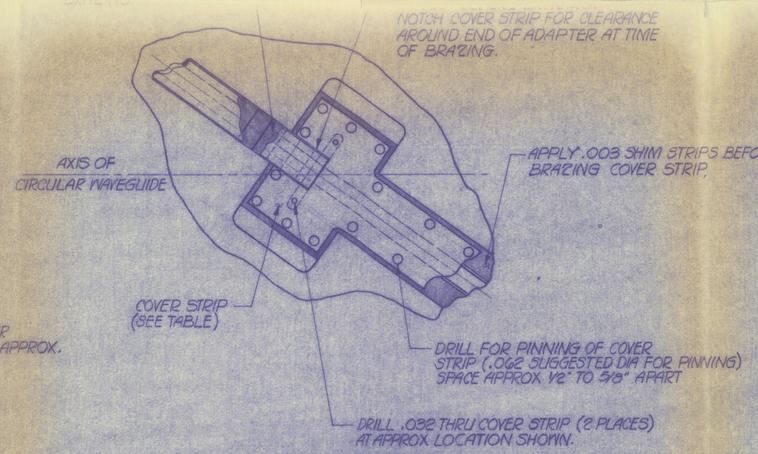

ENLARGED VIEW AT A

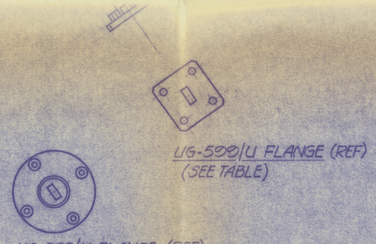

NOTES:

1. VENDOR INFORMATION:
   A COPY OF DWG. B1331OM17 TO ACCOMPANY THIS THIS ASSEMBLY WITH EACH PROCUREMENT.
2. 2. AFTER BRAZING OPERATION IS COMPLETE AND ASSY THOROUGHLY CLEANED OF FLUX, BRING TO "T4" HARDNESS.

D1331OM25	
NEXT ASSY	USED ON

UNLESS OTHERWISE SPECIFIED DIMENSIONS ARE IN INCHES
TOLERANCES: ANGLES ±
3 PLACE DECIMALS (.XXX): ±
2 PLACE DECIMALS (.XX): ±
1 PLACE DECIMALS (.X): ±

MATERIAL:

FINISH:

PROJECT: VLA

TITLE: COUPLER BRAZING ASSEMBLY

NATIONAL RADIO ASTRONOMY OBSERVATORY
CHARLOTTESVILLE, VA. 22901

DRAWN BY TMETLINE	DATE 12/2/15
DESIGNED BY	DATE
APPROVED BY	DATE

SHEET NUMBER | DRAWING NUMBER D1331OM25 | REV. | SCALE 1/1

BRUNING 40-22 24984

REV.	DATE	DRAWN BY	APPRV'D BY	DESCRIPTION

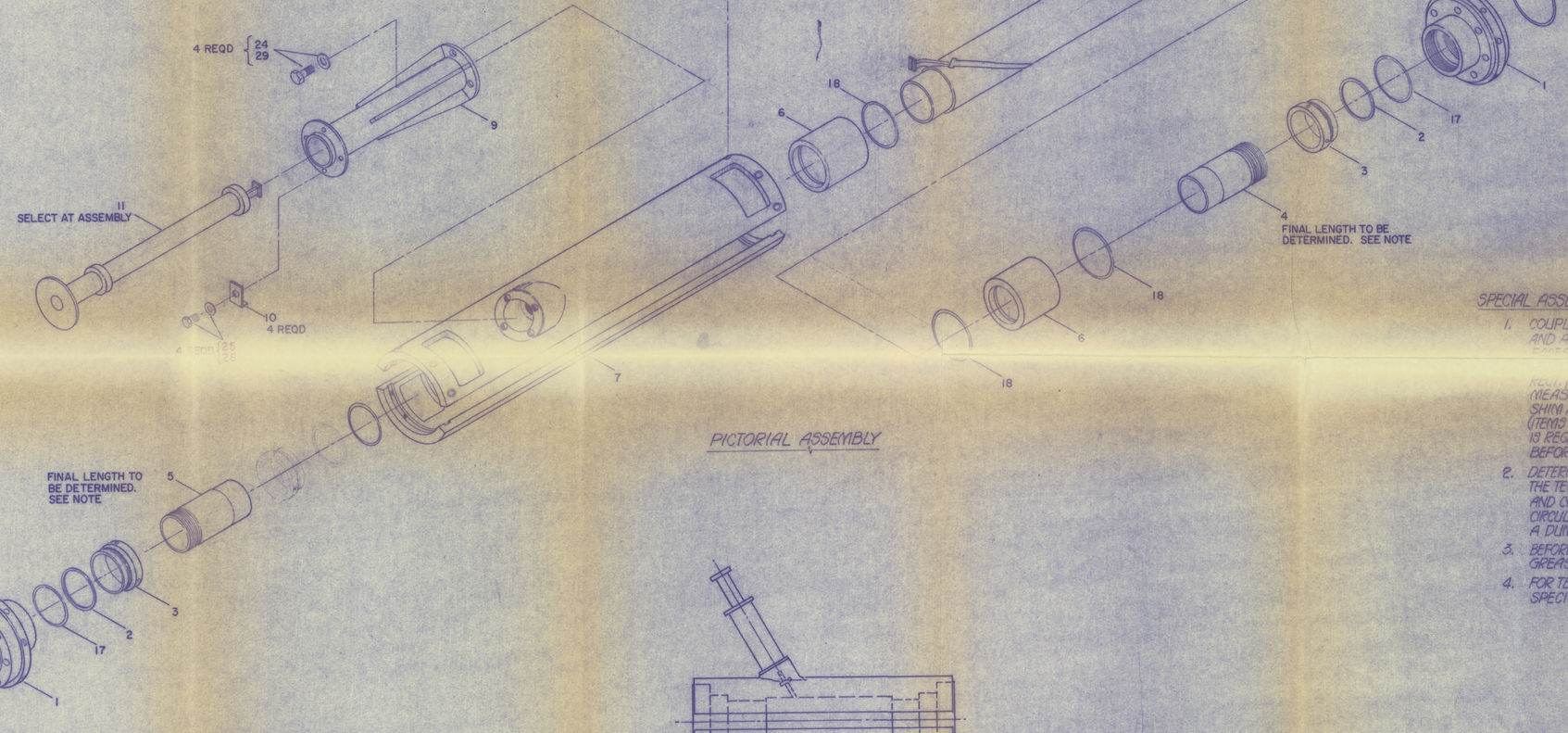

PICTORIAL ASSEMBLY

SPECIAL ASSEMBLY INSTRUCTIONS

1. COUPLER BRAZING ASSEMBLY, ITEM 8, TO BE POSITIONED AND ADJUSTED TO CORRECT LENGTH WITH THE OUTSIDE FACE OF FLANGE OF PART NUMBER 01-[illegible] (ITEM 11) SHOULD BE CAREFULLY MEASURED AND NOTED. [illegible] FINAL INSTALLATION OF INTERFACE SHIM, ITEM 12. THE LENGTHS OF (2) 60MM WAVEGUIDE PIECES (ITEMS 4 AND 5) TO BE DETERMINED AND NOTED. IF MACHINING IS REQD FOR ITEMS 4,5 AND 12 IT SHOULD BE DONE AND INSTALLED BEFORE ASSY SETUP IS DISMANTLED.
2. DETERMINE THE CHARACTERISTICS OF COUPLE, ITEM 8, BY USING THE TEST DATA AVAILABLE IN N.R.A.O. AND CHOOSE W.G. PORT A OR B AS THE ONE TO MATE WITH RECT./CIRCULAR W.G. ITEM 11. THE OTHER PORT TO BE PLUGGED WITH A DUMMY LOAD, ITEM 13.
3. BEFORE INSTALLING 'O'-RINGS, APPLY A THIN COATING OF SILICONE GREASE, ITEM 16, TO SURFACES OF 'O' RINGS.
4. FOR TESTING AND CALIBRATION REQUIREMENTS, REFER TO SPECIFICATION

FOR PARTS LIST, REFER TO A1332021

NEXT ASSY	USED ON

UNLESS OTHERWISE SPECIFIED DIMENSIONS ARE IN INCHES
TOLERANCES: ANGLES ±
3 PLACE DECIMALS (.XXX): ±
2 PLACE DECIMALS (.XX): ±
1 PLACE DECIMALS (.X): ±
MATERIAL:
FINISH:

INTERPRET

NATIONAL RADIO ASTRONOMY OBSERVATORY
CHARLOTTESVILLE, VA. 22901

COUPLER SUPPORT ASSEMBLY (60MM WAVEGUIDE)

DRAWN BY HARTLINE	DATE 1/26/73	
DESIGNED BY	DATE	
APPROVED BY	DATE	
SHEET NUMBER	DRAWING NUMBER D1332060	REV.

SCALE ~

BRUNING 40-22 24984